NASA Contractor Report 159092

NASA-CR-159092

1979 00 20608

Evaluation of the Spatial and Temporal Measurement Requirements of Remote Sensors for Monitoring Regional Air Pollution Episodes

Hsiao-hua K. Burke
Clinton J. Bowley
James C. Barnes

ENVIRONMENTAL RESEARCH & TECHNOLOGY, INC.
696 Virginia Road
Concord, Massachusetts   01742

NASA

National Aeronautics and
Space Administration

Langley Research Center
Hampton, Virginia 23665
AC 804 827-3966

NASA Contractor Report 159092

N79-28799#

Evaluation of the Spatial and Temporal Measurement Requirements of Remote Sensors for Monitoring Regional Air Pollution Episodes

Hsiao-hua K. Burke
Clinton J. Bowley
James C. Barnes

ENVIRONMENTAL RESEARCH & TECHNOLOGY, INC.
696 Virginia Road
Concord, Massachusetts 01742

NASA

National Aeronautics and
Space Administration

Langley Research Center
Hampton, Virginia 23665
AC 804 827-3966

FOREWORD

ABSTRACT

This study was performed to evaluate the spatial and temporal measurement requirements of satellite sensors for monitoring regional air pollution episodes. The study made use of two sets of data from the Sulfate Regional Experiment (SURE), which has provided the first ground-based aerosol measurements from a regional-scale station network. The sulfate data were analyzed for two air pollution episode cases: 19-23 July 1978 and 3-5 August 1977. In addition to the empirical data analysis, computations were made using a simulation model. A cursory evaluation of existing sensor systems was also performed with regard to these measurement requirements.

The results of the analysis indicate that the key considerations required for episode mapping from satellite sensors are the following: (a) detection of sulfate levels exceeding 20 $\mu g/m^3$; (b) capability to view a broad area (of the order of 1500 km swath) because of regional extent of pollution episodes; (c) spatial resolution sufficient to detect variations in sulfate levels of greater than 10 $\mu g/m^3$ over distances of the order of 50 to 75 km; (d) repeat coverage at least on a daily basis; and (e) satellite observations during the mid to late morning local time, when the sulfate levels have begun to increase after the early morning minimum levels, and convective-type cloud cover has not yet increased to the amount reached later in the afternoon; analysis of the satellite imagery has shown that convective clouds can obscure haze patterns. Additional parameters based on spectral analysis include wavelength and bandwidth requirements.

TABLE OF CONTENTS

1. INTRODUCTION

1.1 Purpose and Objectives

This study was performed for the National Aeronautics and Space Administration (NASA) Langley Research Center (LaRC) by Environmental Research & Technology, Inc. (ERT). The purpose of the study was to evaluate the spatial and temporal measurement requirements of remote sensors for monitoring regional air pollution episodes.

Several types of instruments designed to measure air pollution from space are in varying degrees of development and testing. In general, these sensors are designed to measure the total burden of pollution species over a relatively large field-of-view (30 to 100 km) along the spacecraft groundtrack. These instruments have not yet been flown in space, or in many instances, even tested on aircraft platforms. Moreover, until recently there has been no suitable air quality data base available for evaluating the spatial and temporal resolution requirements of a satellite monitoring system.

A comprehensive sulfate measurement program was established in 1977 because of concern with atmospheric pollution and pollutant transport on a regional scale. This program, known as the Sulfate Regional Experiment (SURE), is funded by the Electric Power Research Institute (EPRI), coordinated with the Environmental Protection Agency (EPA) and the Department of Energy (DOE). The SURE data base has provided the first ground-based aerosol measurements which are suitable for evaluating the requirements for spatial and temporal measurements.

The specific objectives of the study were to: (1) define air pollution episodes; (2) select pollution episode cases for analysis from the SURE data base; (3) determine the spatial and temporal resolution requirements of remote sensors using the empirical and/or modeled SURE data, including the impact of varying degrees of cloudiness; (4) rank the most important parameters required for mapping pollution episodes; and (5) perform a cursory evaluation of the use of an existing sensor system for regional pollution monitoring.

1.2   Review of Previous Studies

In another recently completed study for NASA/LaRC (Barnes et al, 1979), the capabilities of satellite imagery for monitoring regional air pollution episodes were evaluated. In the introductory section of that report, earlier studies of the use of satellite data to detect atmospheric aerosols are described. The earlier studies include those reported by Prospero, et al (1970), McLellan (1971), Lyons and Northouse (1973), and Griggs (1973). Later studies include Brown and Karn (1976), Fraser (1976), Husar, et al (1976), Lyons and Husar (1976), Bowley, et al (1977), and Griggs (1978).

In the study by Barnes et al (1979), the SURE measurements were used as correlative data to evaluate various existing sensor systems, including NOAA/VHRR (Very High Resolution Radiometer), GOES (Geostationary Operational Environmental Satellite), and Landsat. The results of the analysis of three cases, each representing a significant pollution epi-sode (based on low reported visibilities and high sulfate levels), showed that when a regional air pollution episode has built up over a period of three to five days to a point where sulfate levels of ≥ 30 micrograms per cubic meter ($\mu g/m^3$) are being measured, a haze pattern that correlates closely with the area of reported low surface visibilities ($\leq$ four miles) and high sulfate levels can be detected in satellite visible-channel imagery. The extent and transport of the haze pattern can be monitored from the satellite data over the period of the maximum intensity of the episode. In the other cases, with lower levels of sulfate being measured, the haze patterns are more difficult to detect in the imagery.

In addition to the analysis of the satellite imagery, the feasibility of detecting pollution episodes from space was investigated using a sim-ulation model. The results indicated that it is possible to monitor both the magnitude and areal extent of pollution episodes. Quantitative infor-mation on total aerosol loading derived from an analysis of satellite digitized data using an atmospheric radiative transfer model agreed well with the results obtained from surface measurements.

2. SELECTION OF EPISODE CASES

2.1 Criteria for Defining Pollution Episodes

Studies of the occurrence of atmospheric aerosols in the eastern United States, particularly the distribution of airborne particulate sulfates, have been discussed in several reports, including EPA (1974, 1975), Tong et al (1976), Hidy et al (1977), Tong and Batchelder (1978), and Mueller et al (1979). In the paper by Hidy et al (1977), it is pointed out that sulfate is of concern because of the epidemiological allusion to possible adverse effects to human health and welfare, the occurrence of acid precipitation, and visibility impairment in the eastern United States. These authors also hypothesize that the regional sulfate distributions observed in the eastern United States are related to the cumulative impact of major sources closely spaced along a direction parallel to the prevailing wind and atmospheric accumulation during long range transport.

Despite the concern about sulfates, regulatory standards, at the federal level, directed toward the control of atmospheric sulfates have not been promulgated because of the lack of a sufficient technical data base (Tong et al, 1976). At that time, ambient sulfate standards had been established in only five states, with California, for example, setting a standard of 25 $\mu g/m^3$ for a 24-hour average.

Using measurements collected during 1974, Tong and Batchelder (1978) found the geographical distribution of 24-hour ambient sulfate levels in the eastern United States to range from less than 1 $\mu g/m^3$ in remote areas to greater than 60 $\mu g/m^3$ in heavily industrialized urban areas; the peak sulfate levels tend to occur during summer months. In an initial analysis of SURE data collected in August and October 1977 and mid-January to mid-February 1978, Mueller et al (1979) also found that the 24-hour sulfate concentrations tended to be greatest in summer but levels in excess of 20 $\mu g/m^3$ also occurred in winter. Moreover, the frequency distributions of sulfate concentrations in urban and rural locations were not significantly different. The recent SURE data (August 1977 through July 1978) indicate that 24-hour sulfate concentrations exceed 6 $\mu g/m^3$ 50% of the time, 10 $\mu g/m^3$ about 30% of the time, and 20 $\mu g/m^3$ 5% of the time.

As summarized by Mueller et al (1979), the early results of studies such as those described above using data primarily from the summer months, have indicated that regional hazes occur in multiday episodes that involve synoptic scale stagnation conditions with inflow of maritime tropical air into the eastern and mid-western United States. Sulfate is a major component of the particles in these hazes, and therefore, continues to be of considerable interest. Although no distinct criteria have been established to describe a critical air pollution episode, a sulfate level ≥ 20 $\mu g/m^3$ describes a "well-defined haze episode" (Mueller et al, 1979). For purposes of this study, therefore, pollution episodes have been defined as those with sulfate levels ≥ 20 $\mu g/m^3$.

2.2 Description of SURE Data Base

Some ground-based aerosol measurements applicable to regional-scale studies were collected for 1974 from the EPA's National Aerometric Data Bank (NADB) and the Tennessee Valley Authority (TVA), as well as from the National Air Sampling Network (NASN) stations. The sulfate measurements taken at all stations consisted of 24-hour average values obtained by chemical analysis of high volume particulate filters. The network of stations at that time was not adequate, however, to carry out thorough regional-scale studies.

The much more comprehensive Sulfate Regional Experiment (SURE) measurement program was undertaken in 1977 (Mueller, et al, 1979). The purpose of SURE, sponsored by the Electric Power Research Institue, was to establish an extensive data base on the mass concentration, size distribution and chemical composition of the atmospheric particulate matter in the nonurban eastern United States for several seasons. Data have been acquired from a 54 ground station network from August 1977 through October 1978, and from aircraft during six days of flying during one month each season. The area covered by the SURE is approximately 2400 km x 1840 km from eastern Kansas to the Atlantic Coast, and from mid-Alabama to southeastern Canada. The SURE station network is shown in Figure 2-1.

The ground monitoring network for the SURE consists of nine Class I stations and 45 Class II stations. The Class I stations were instrumented to operate continuously from August 1977, measuring SO_2, particulate mass, NO/NO_x, O_3, sulfate, nitrates and other supplemental parameters such as
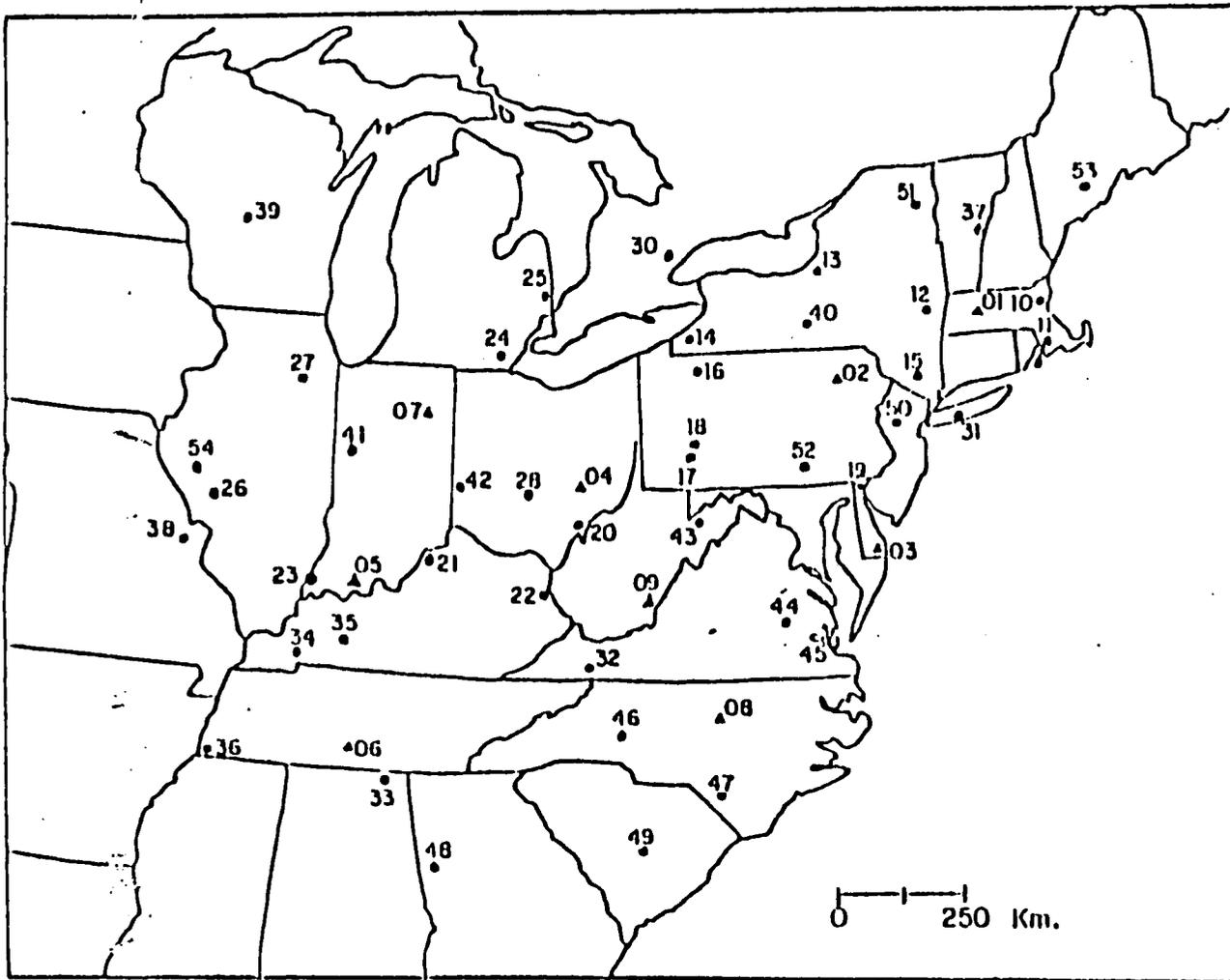
Figure 2-1   SURE Region Showing Locations and Numbers of the Ground
Measurement Stations. Triangles are the Class I Stations;
the Circles are Class II Stations

hydrocarbons and trace metals. Sulfates have been measured to provide 24-hour averages daily. Sulfates have also been measured in small particles (≤ 3 µm) in 3-hour averages during the central month for each season of the SURE period to delineate the diurnal variations.

The Class II stations have been operated for only the central month of each season. Parameters measured are SO_2 and 24-hour average sulfate and particulate mass concentrations. The intensive measurement months were August and October 1977, and January, April, July and October 1978.

In addition to these air quality measurements, supporting meteorological data have also been obtained from existing National Weather Service (NWS) observing stations throughout the eastern half of the United States. The meteorological data consist of hourly AIRWAYS synoptic observations, as well as radiosonde soundings and pilot balloon soundings.

2.3 Cases Selected for Analysis

The selection of cases for analysis was based on the presence of high sulfate levels over the eastern United States as reported by the SURE network during the intensive data gathering months. Examination of all of the SURE synoptic sulfate maps during these intensive data gathering months showed that the peak regional sulfate episodes occurred during the August 1977 and July 1978 periods. Based on the review of the sulfate measurements, two cases were selected for analysis: (1) 19-23 July 1978; and (2) 3-5 August 1977. These cases, along with an earlier case (1974), were also analyzed in the recently completed study for NASA/LaRC by Barnes et al (1979).

The characteristics of these two episodes are described briefly below. The spatial and temporal characteristics of the sulfate distributions are analyzed in detail in Section 3. The July 1978 episode is discussed first because of better satellite data available during that period.

2.3.1 Case 1: 19-23 July 1978

The synoptic weather pattern over the Northeast during the period of 19-23 July 1978 was typical of the summertime conditions associated with observed haze episodes. A large stationary high pressure cell became established off the mid-Atlantic coast by 19 July. The clockwise

6

circulation around this system brought tropical air northward into much of the Northeast on light to moderate southerly surface wind flow. Maximum daytime temperatures reached 32-35°C (upper 80's to mid 90°F), with dewpoint temperatures of 22-24°C (low to mid 70's°F) resulting in extremely high humidity. Widespread haze, smoke and light fog restricting the surface visibilities were reported throughout much of the Northeast.

The preliminary SURE data indicated high sulfate levels over the northeastern United States during this period. Maximum 24-hour average values (preliminary, unvalidated measurements) ranged as high as 40 to 50 $\mu g/m^3$ on 22 July. Throughout the pollution episode, a close relationship existed between the area of reduced surface visibility in haze, smoke and light fog and the area of peak sulfate concentrations.

2.3.2 Case 2: 3-5 August 1977

The meteorological conditions over the northeastern part of the country during the period 3-5 August 1977 were also similar to other verified haze episodes. During this period, the Burmuda High was nearly stationary and was intensifying off the East Coast. The circulation around this system caused light southerly surface wind flow over much of the eastern third of the country, with warm, humid tropical air advecting northward into the Ohio Valley region, then eastward into New England. The development of reduced visibility areas (< 4 miles) in haze and light fog and their eventual transport into New York state and New England is well documented on visibility maps for each day of the pollution episode.

The SURE data (unvalidated measurements) showed that the episode began on 3 August as peak sulfate levels (24-hour averages) ranged from 20 to 26 $\mu g/m^3$ over the Ohio Valley region. By 4 August, peak sulfate levels ranged from 25 to 34 $\mu g/m^3$ over Pennsylvania, southern New York state, and central New England. Sulfate levels lessened somewhat on 5 August, with peak concentrations of 20 to 24 $\mu g/m^3$ elongated east-west from central New England westward into the eastern Great Lakes region.

3. ANALYSIS OF SPATIAL AND TEMPORAL
CHARACTERISTICS OF SELECTED EPISODE CASES

A more detailed description of the two selected episodes is presented in this section. The emphasis is on the spatial and temporal character-istics based on analysis of the SURE data. The total duration of the episodes, the variation in daily maximum sulfate levels, variations over 3-hour time periods (when 3-hour averages are available), daily areal extents of the episodes, as well as gradients of the sulfate levels, are discussed. It should be noted that some of the SURE measurements are unvalidated; nevertheless, the accuracy and extent of the measurements are, in general, sufficient for the purposes of this study. The July 1978 case, for which a more complete satellite data sample was available, is discussed first.

3.1 Case 1: 19-23 July 1978

3.1.1 Temporal Characteristics of Sulfate Distribution

The analyses of 24-hour average sulfate levels across the SURE dat-network show that the episode began on 19 July and lasted through 23 July. Analyses of 24-hour average sulfate levels ($\mu g/m^3$) shown in Figures 3-1 through 3-5, show a gradual eastward transport during the five-day period. On 19 July (Figure 3-1) an elongated (east-west) band of elevated sulfate levels (20 to 28 $\mu g/m^3$) stretched from Illinois to the coastal region south of New England. Also, a small pocket with levels ranging from 30 to 40 $\mu g/m^3$ was located over the region of eastern Lake Erie. By 20 July (Figure 3-2) the elongated band of elevated sulfate levels (20 - 30 $\mu g/m^3$) became oriented more WSW to ENE from the area of southern Indiana into central New England, while the band of maximum levels between 30 to 40 $\mu g/m^3$ was elongated SW to NE along the eastern Great Lakes region. Little change in the SURE sulfate analysis was noted on 21 July (Figure 3-3). On 22 July (Figure 3-4) the area of peak 24-hour average sulfate levels, which had increased to from 40 to 55 $\mu g/m^3$, was now located well south-east of the eastern Great Lakes region, over southern New Jersey, Delaware and Maryland. By 23 July (Figure 3-5) the maximum levels were located well off the coastal region from southern New England to Delaware, with levels ranging from 25 to 35 $\mu g/m^3$ along the immediate coast.
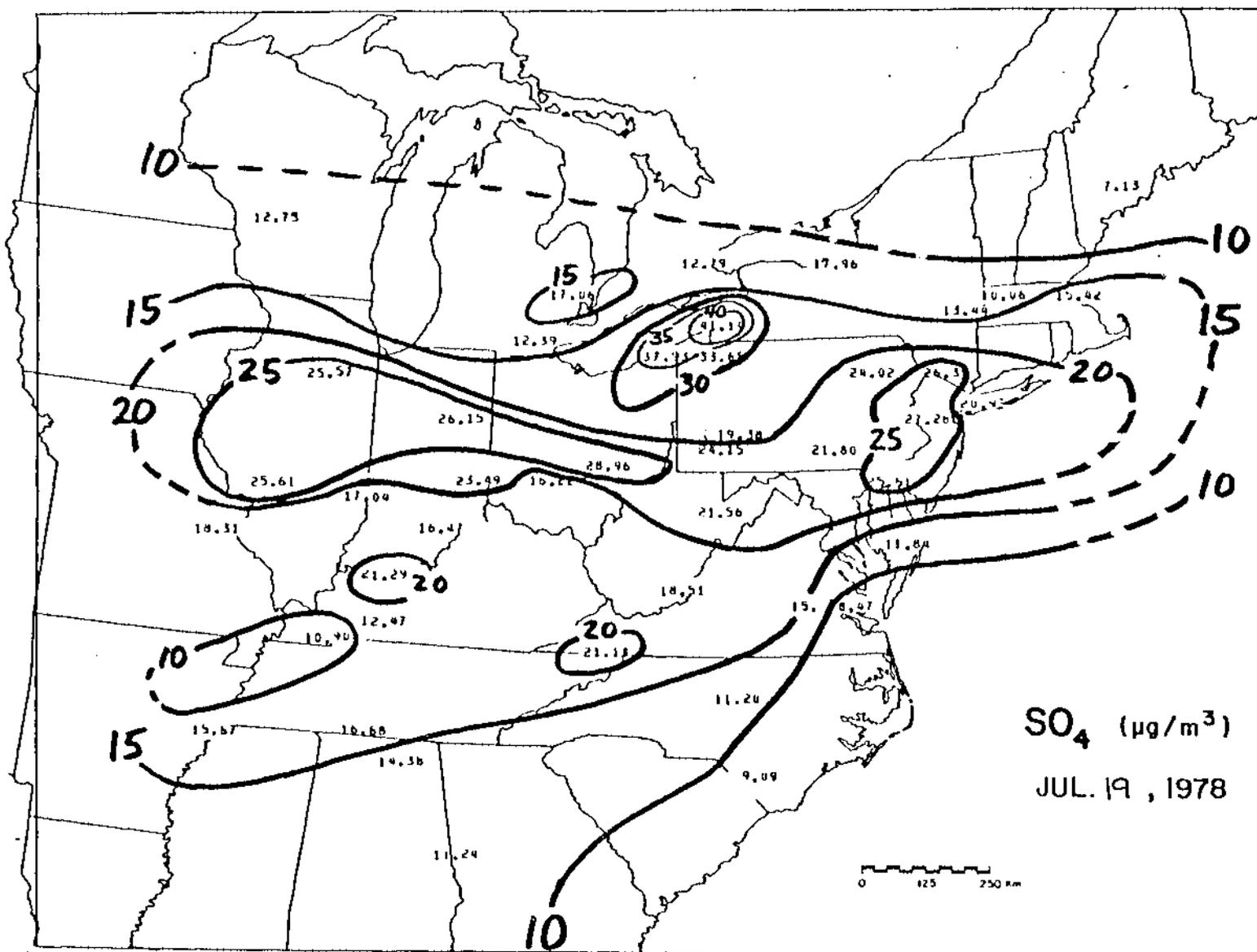
Figure 3-1   Analysis of 24-Hour Average Sulfate Measurements ($\mu g/m^3$) from the SURE Data Network for 19 July 1978
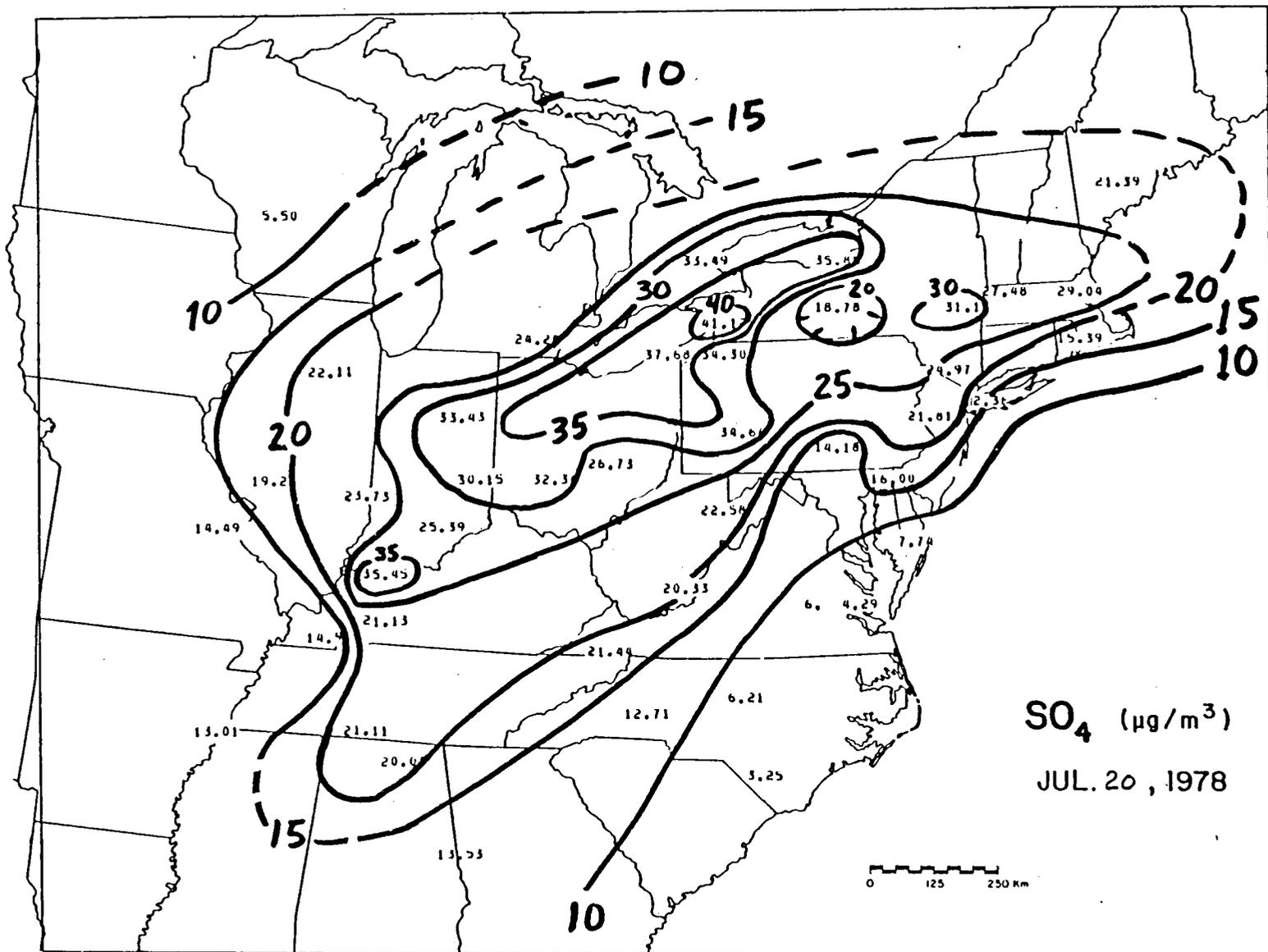
Figure 3-2   Analysis of 24-Hour Average Sulfate Measurements (μg/m³) from
the SURE Data Network for 20 July 1978
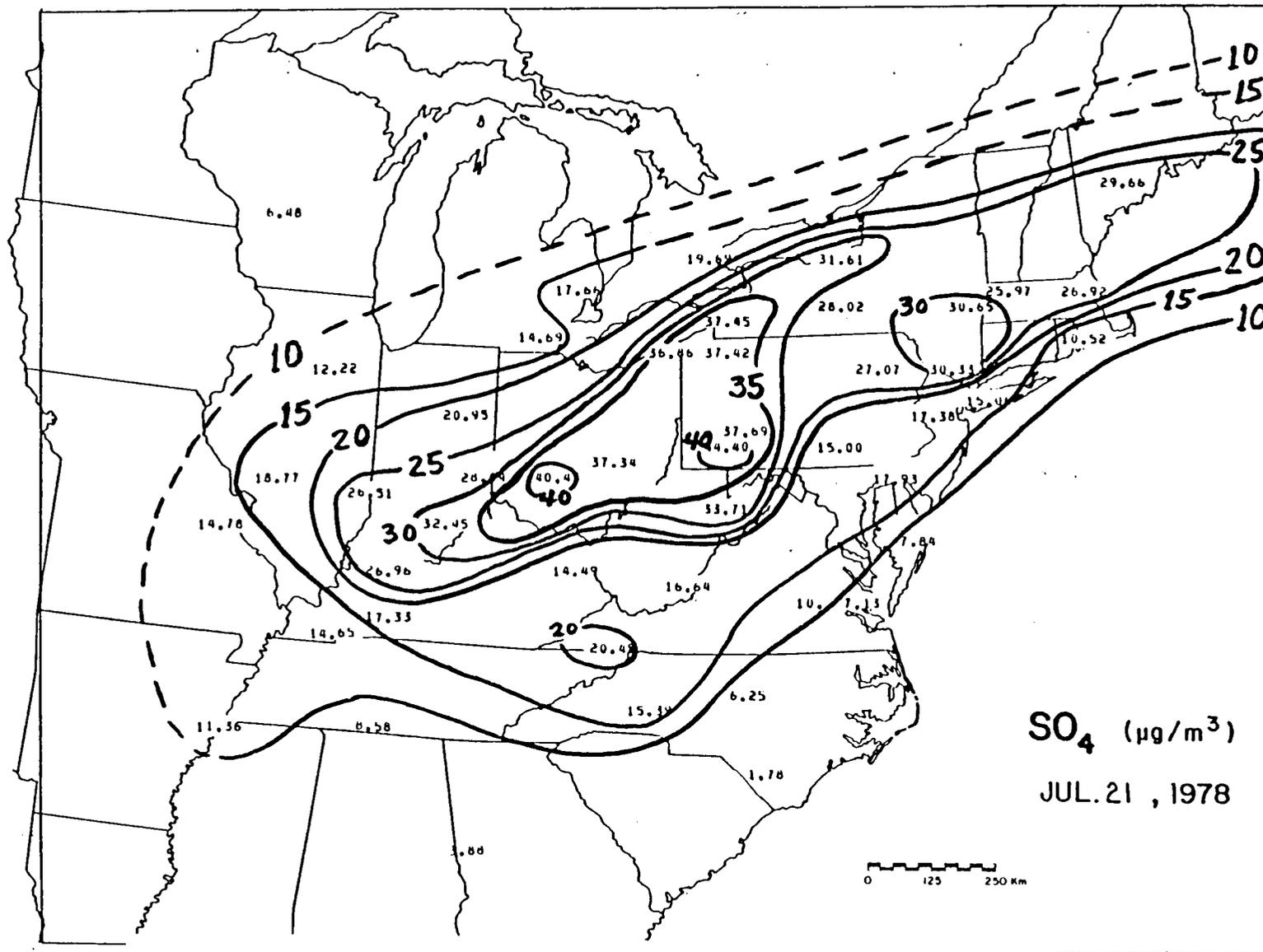
Figure 3-3   Analysis of 24-Hour Average Sulfate Measurements ($\mu g/m^3$) from the SURE Data Network for 21 July 1978
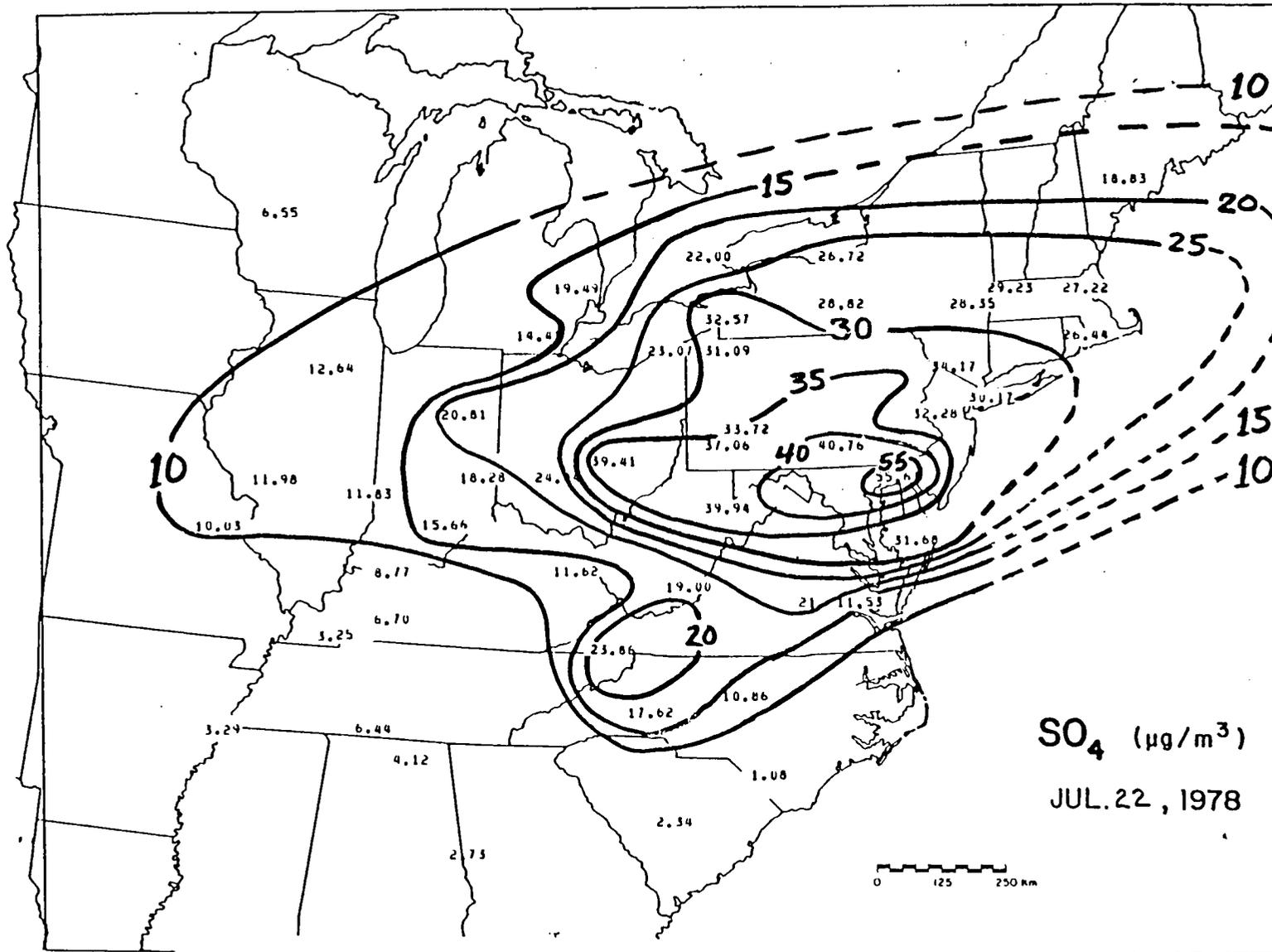
Figure 3-4   Analysis of 24-Hour Average Sulfate Measurements ($\mu g/m^3$) from the SURE Data Network for 22 July 1978

2.74

4.09

16.81

5.43

16.90

23.37   29.94

13.35   14.59   15.17   25.03   35   30

14.49

12.46

5.02

5.73   17.33   32.87   31.19   25   20

5.73   17.54   21.70

15
17.93

6.84   6.54   9.04   20.58   35
6.25   9.07   34.48
35.57

6.22

16.94   10.77   15

4.41   20.

3.85   22.41   20

4.05   5.74   5.71

3.65   0.82

1.96

5.98

10   15   20   25   30   20   15   10

SO_4 ($\mu g/m^3$)

JUL. 23, 1978

0   125   250 Km
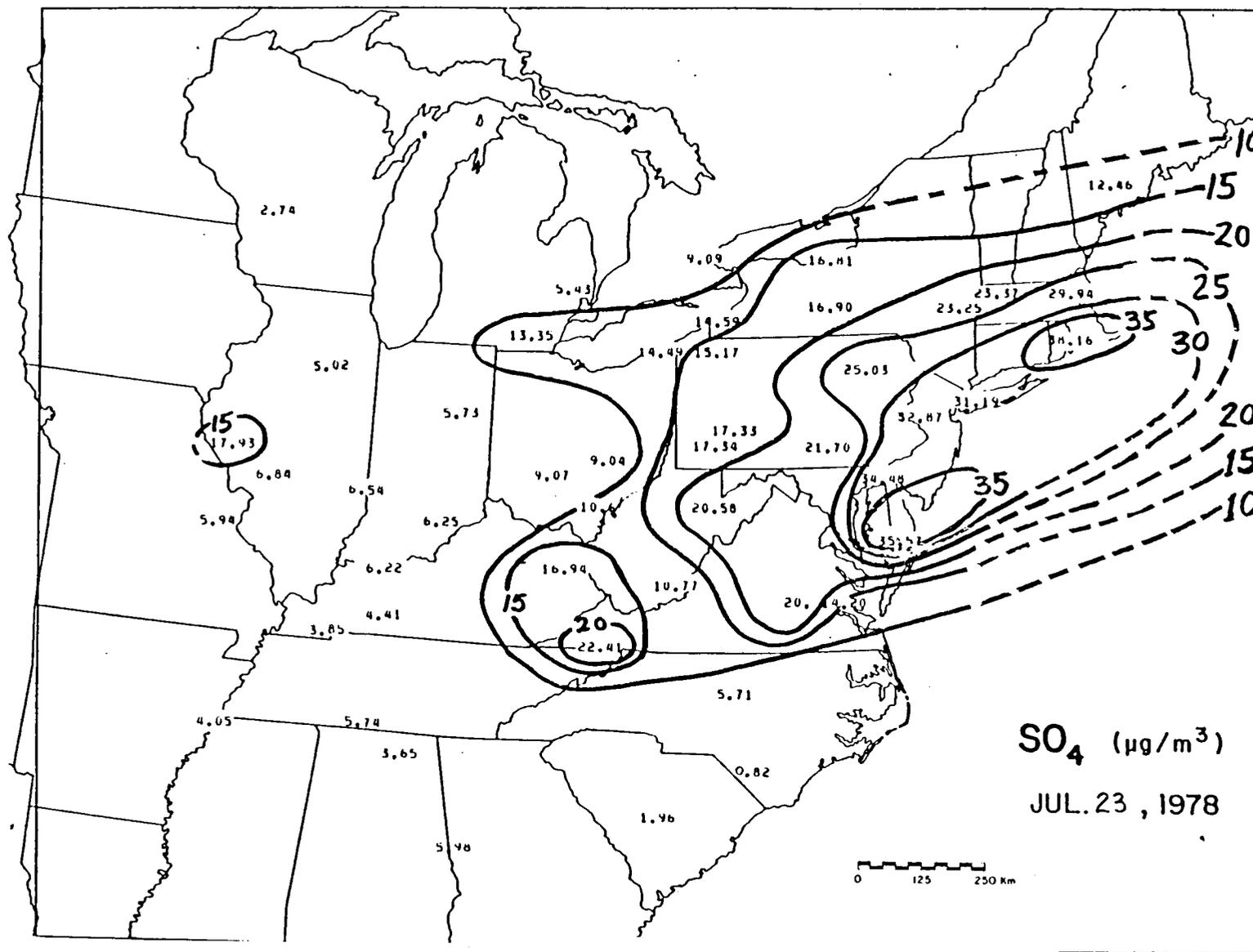
Figure 3-5   Analysis of 24-Hour Average Sulfate Measurements ($\mu g/m^3$) from the SURE Data Network for 23 July 1978

Plots of 3-hour average sulfate levels for selected Class I stations showed considerable diurnal variation throughout the episode. In most instances, the maximum sulfate levels occur between local noon and 1500 LST, whereas minimum levels occur prior to sunrise between 0300 and 0600 LST. The graph of 3-hour average sulfate levels for Duncan Falls, Ohio is shown in Figure 3-6. Each plotted value represents the average at the end of a 3-hour period. On 19 July, high sulfate levels were apparently advected into the region during late evening as levels which had been gradually falling throughout the day, increased significantly after 2100 LST. The diurnal trend of the 3-hour averages behave quite similarly on 20, 21 and 22 July, with a gradual increase each day in maximum levels during the mid-afternoon hours, and gradual increase in minimum levels during the early morning hours. The graph of 3-hourly average sulfate levels for Indian River (Millsboro, Delaware), shown in Figure 3-7, shows a dramatic increase in sulfate levels between 0900 LST and 1500 LST on 22 July. During this period levels increased from 1.2 $\mu g/m^3$ to 60.3 $\mu g/m^3$. As noted earlier in the discussion of the analyses of the 24-hour average sulfate levels, peak levels moved southeastward from the eastern Great Lakes area into the Delware region on this date. Levels gradually decreased to slightly below 20 $\mu g/m^3$ by 0600 LST on 23 July; however, by local noon they had again increased to about 43 $\mu g/m^3$.

3.1.2 Spatial Characteristics of Sulfate Distribution

Analyses of the areal extent of sulfate levels greater than 20 $\mu g/m^3$, derived from plots of 3-hour averages for the nine Class I sites, show a distinct diurnal variation in extent. Analyses were completed for 21 and 22 July for the approximate times of maximum and minimum observed levels (0600 LST and 1500 LST). The analysis for the 3-hour average ending at 0600 LST on 21 July, shown in Figure 3-8, indicates the extent of >20 $\mu g/m^3$ to be approximately 400 km long and 200 km wide in the vicinity of the Kentucky, Indiana and Ohio borders. The analysis for the time of maximum sulfate levels (1200 to 1500 LST), shown in Figure 3-9, reveals a much larger area of >20 $\mu g/m^3$ sulfate levels, extending about 1800 km long and 750 km wide. By 1500 LST, the area of maximum concentration was located about 1000 km northeast of the 0600 LST position. By 22 July, the overall extent at the >20 $\mu g/m^3$ area was much larger at
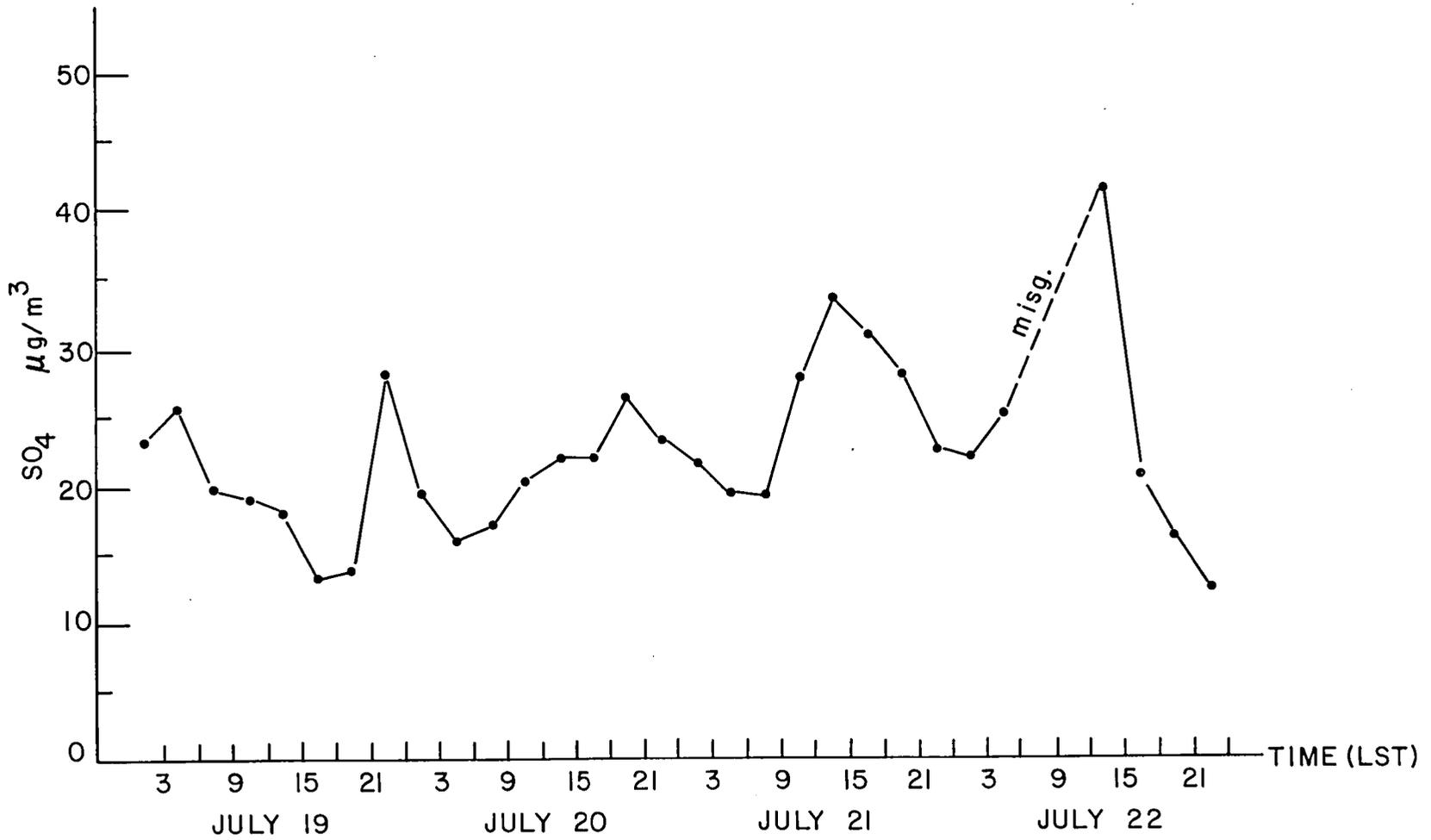
Figure 3-6   Graph Showing 3-Hour Average Sulfate Levels for Duncan Falls, Ohio, 19-22 July 1978. Dashed Line Indicates Missing Data.
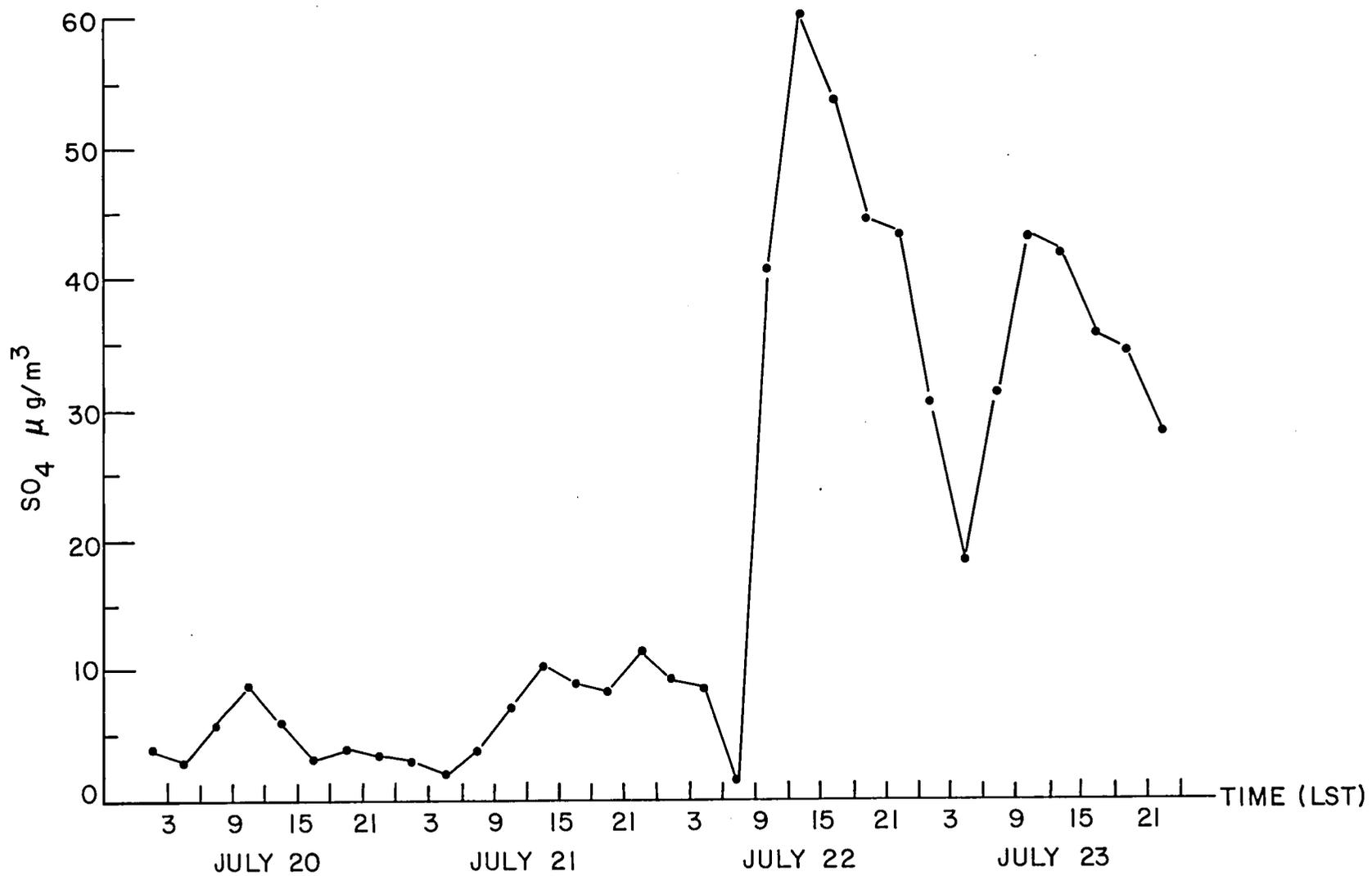
Figure 3-7   Graph Showing 3-Hour Average Sulfate Levels for Indian River, Delaware, 20-23 July 1978
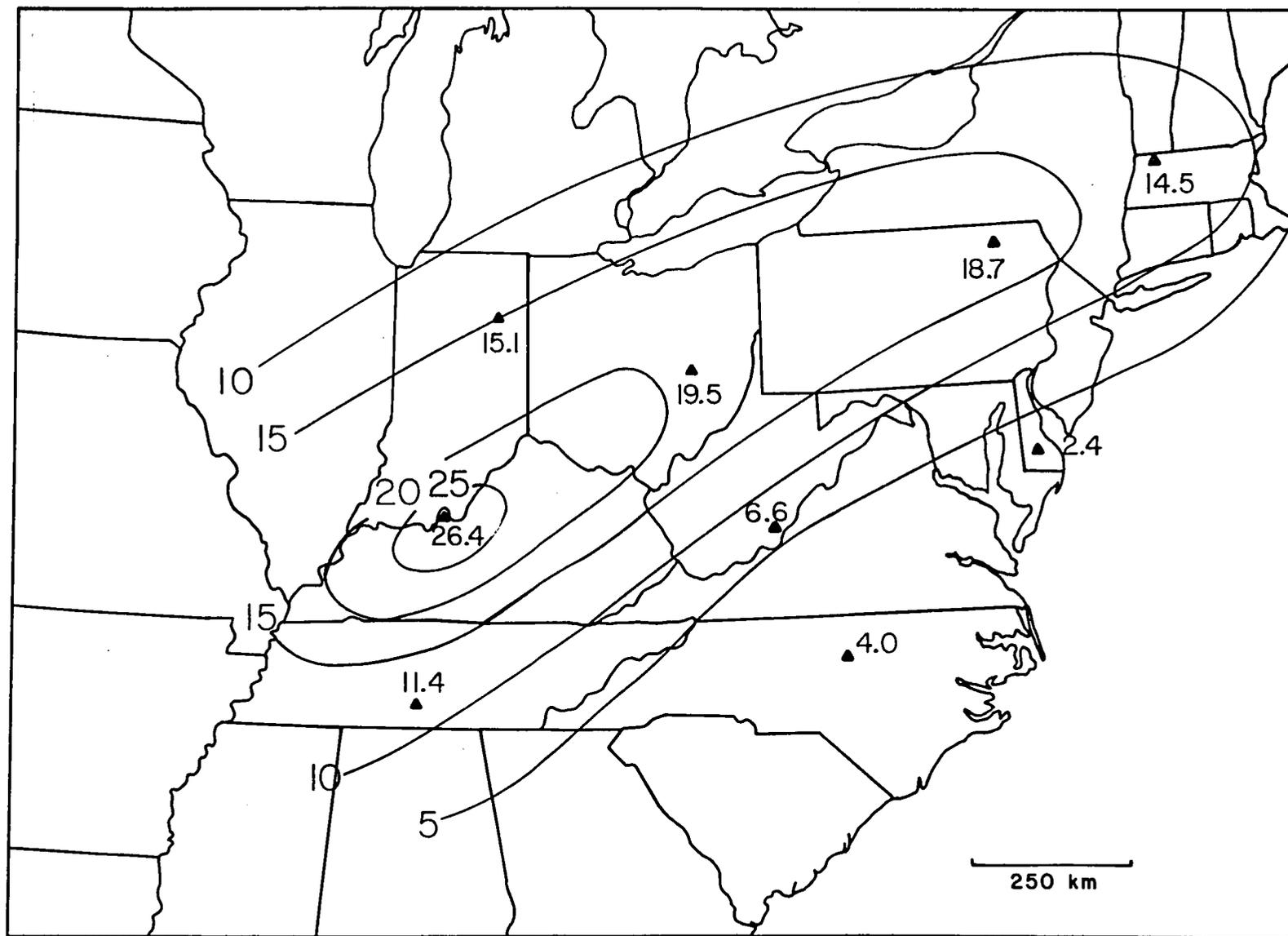
Figure 3-8   Analysis of 3-Hour Average Sulfate Levels (0300-0600 LST), 21 July 1978. Values are in $\mu g/m^3$
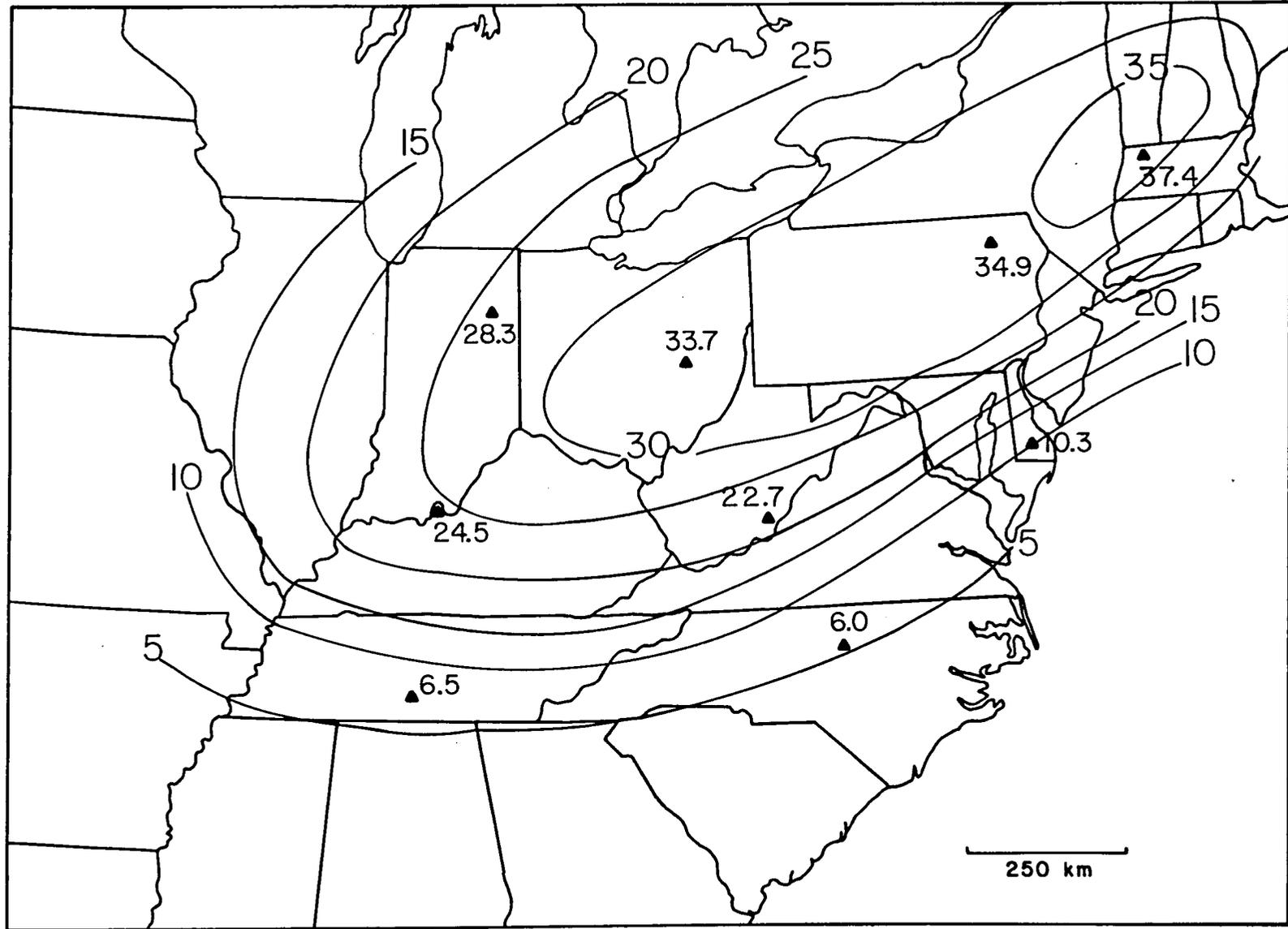
Figure 3-9   Analysis of 3-Hour Average Sulfate Levels (1200-1500 LST), 21 July 1978. Values are in µg/m³

0600 LST than on the previous day; as seen in the analysis shown in Figure 3-10, the extent is about 1500 km long and more than 500 km across. By 1500 LST, the area of maximum concentration was located about 600 km south of the 0600 LST position and the maximum levels had approximately doubled. The eastern extent had moved well off the coast, hence, the length of the area with concentrations >20 $\mu g/m^3$ could not be accurately determined; the width, however, was approximately 750 km (Figure 3-11).

The gradients of the observed sulfate levels were also examined for this episode. As seen in Figures 3-1 through 3-5, the gradients vary greatly from day to day and from location to location. The greatest rates of change of sulfate levels were observed for the latter days of the episode, with the maximum gradients appearing along the southern boundary of the area of high sulfate levels on the 22nd and 23rd. A change of 20 $\mu g/m^3$ over a distance of about 75 km was measured on the 23rd.

3.2 Case 2: 3-5 August 1977

This elevated sulfate episode began on 3 August when maximum 24-hour average levels ranged from 20 to 26 $\mu g/m^3$ across western Pennsylvania, eastern Ohio, and northern West Virginia (Figure 3-12). By 4 August (Figure 3-13), the maximum 24-hour average sulfate levels ranged from 25 to 34 $\mu g/m^3$ across central Pennsylvania, southern New York, and into central New England. The levels subsided somewhat by 5 August (Figure 3-14) into an elongated band of 20 to 24 $\mu g/m^3$ levels extended from just south of Lake Erie, eastward into central New England. This marginally high sulfate episode, therefore, lasted for a total of three days. As the 3-hour average sulfate measurements were not available for this episode, analysis of diurnal variations in the sulfate levels was not possible.

The areal extent of the region experiencing 24-hour average sulfate levels of >20 $\mu g/m^3$ on 3 August was limited to an area 500 km long and about 400 km wide. By 4 August, however, this region expanded considerably. On this date, the band experiencing levels >20 $\mu g/m^3$ measured about 1450 km long, and ranged from 125 to 400 km wide. On 5 August, the extent of the region experiencing these levels measured about 950 km long and 150 km across.

The analyses displayed in Figures 3-12 through 3-14, also reveal
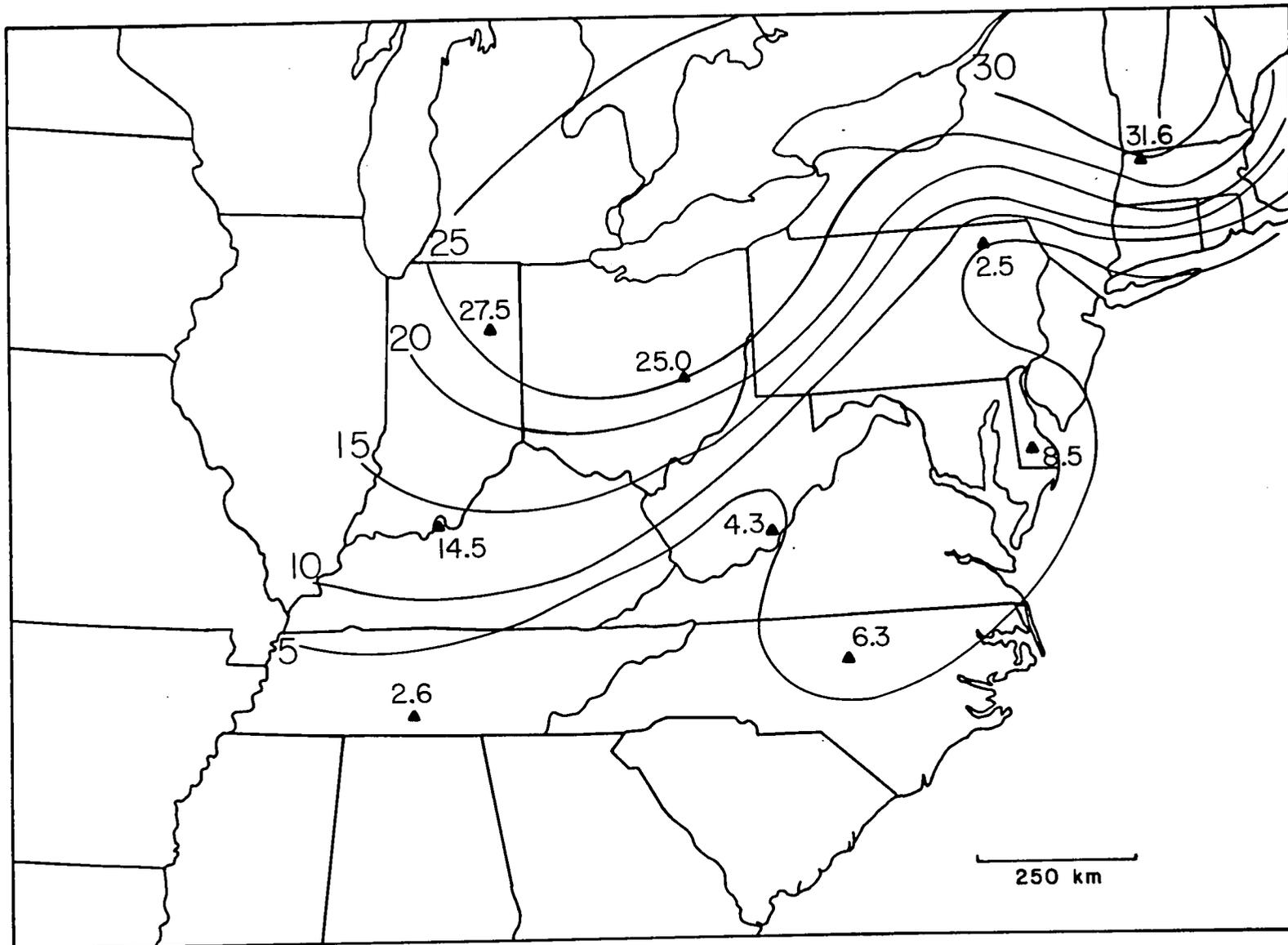
Figure 3-10   Analysis of 3-Hour Average Sulfate Levels (0300-0600 LST), 22 July 1978.
Values are in μg/m³
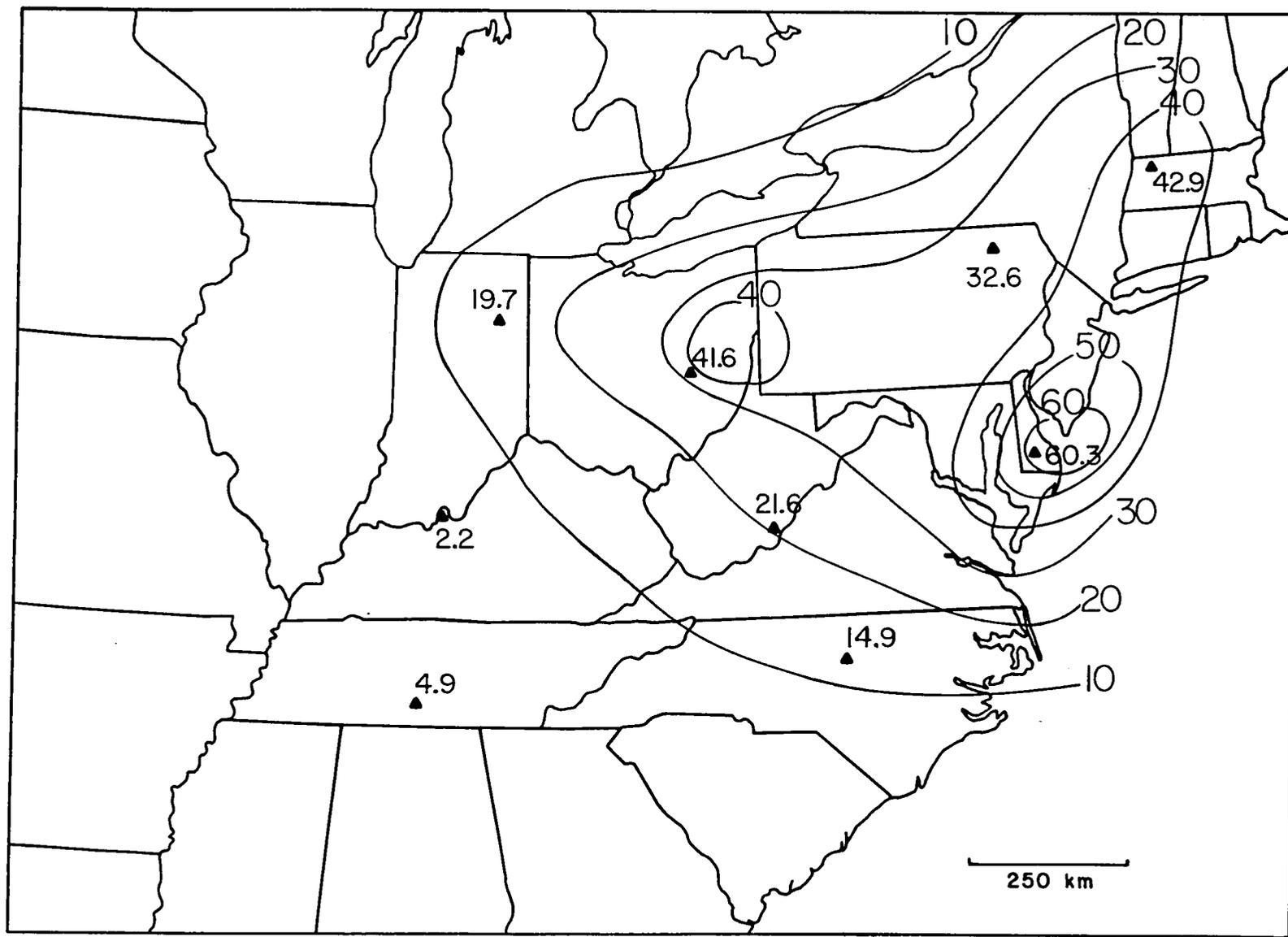
Figure 3-11   Analysis of 3-Hour Average Sulfate Levels (1200-1500 LST), 22 July 1978. Values are in $\mu g/m^3$
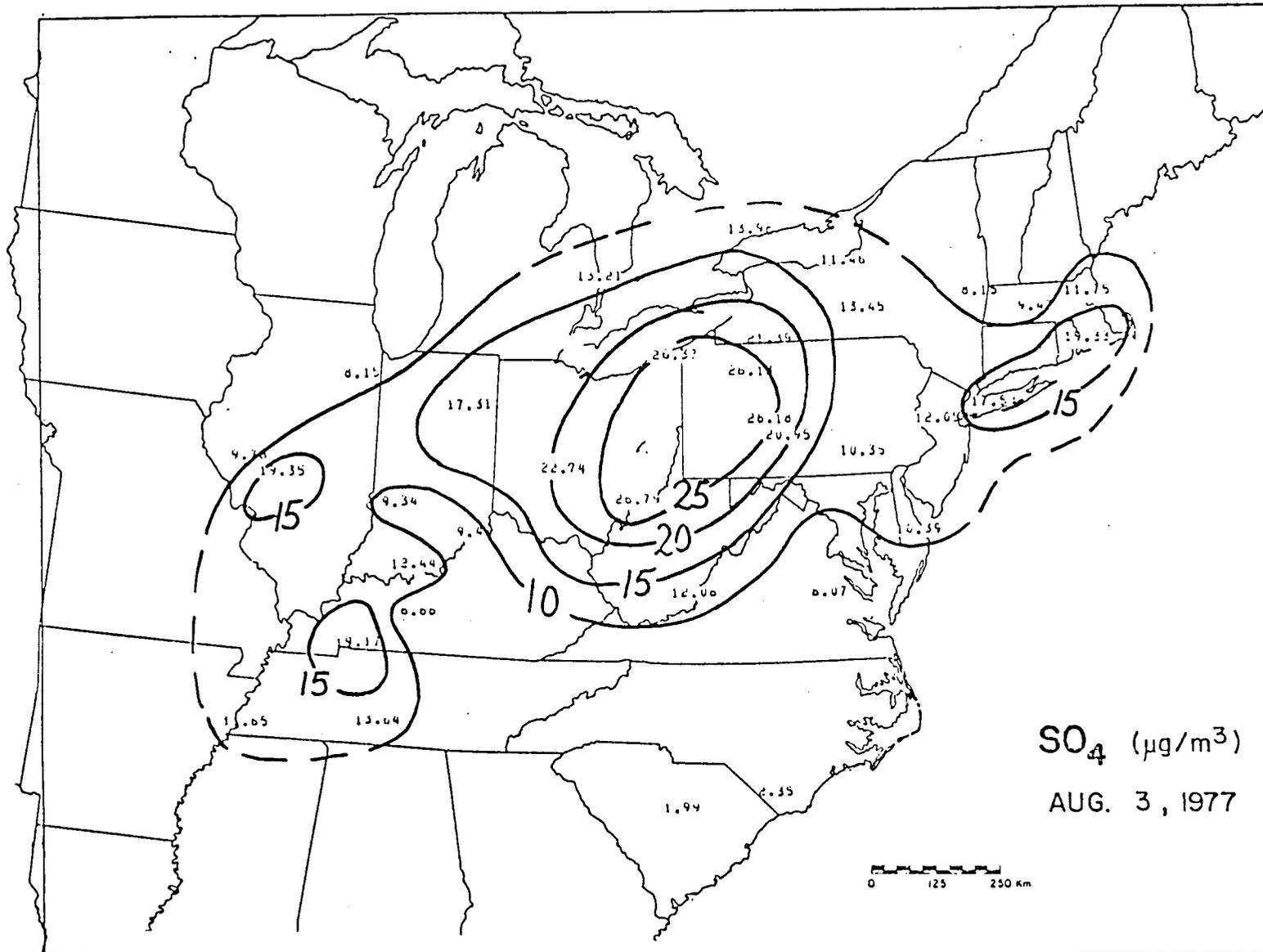
Figure 3-12   Analysis of 24-Hour Average Sulfate Measurements (μg/m³)
from the SURE Data Network for 3 August 1977
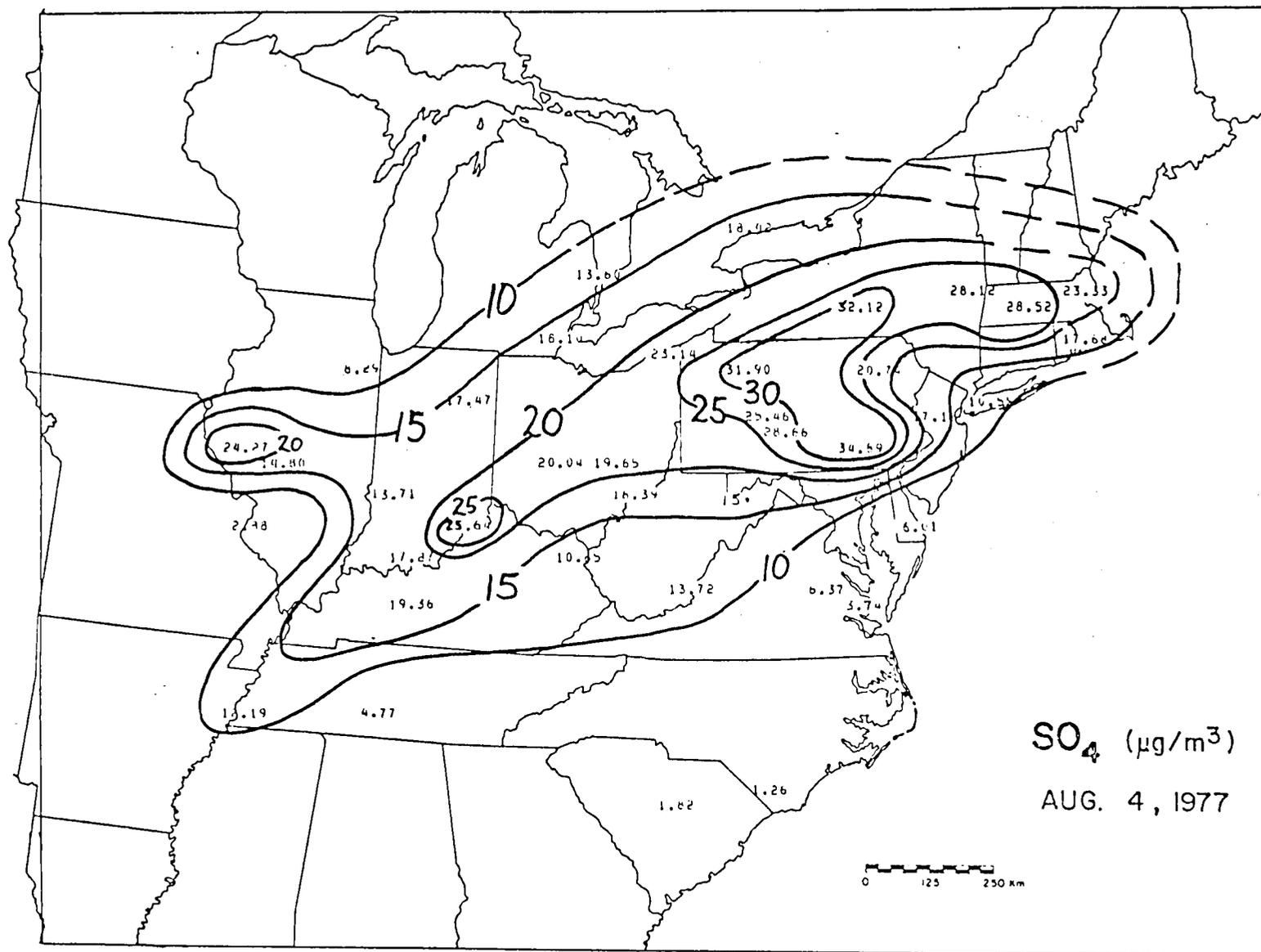
Figure 3-13   Analysis of 24-Hour Average Sulfate Measurements (μg/m³)
from the SURE Data Network for 4 August 1977

Figure 3-14   Analysis of 24-Hour Average Sulfate Measurements (μg/m³)
from the SURE Data Network for 5 August 1977

that the gradients of the sulfate levels were, for the most part, uniformly low on 3 and 5 August. However, on 4 August, a change of 20 $\mu g/m^3$ was measured in the vicinity of southern Pennsylvania and Delaware over a distance of only 75 km; this gradient is approximately the same as the maximum gradient measured in the July 1978 case.

4. ANALYSIS OF EMPIRICAL AND MODELED SATELLITE DATA

4.1 Detection of Haze Patterns in Existing Satellite Imagery

In the study by Barnes et al (1979) the detection of haze patterns associated with pollution episodes by existing satellite imagery systems was investigated. The satellite data analyzed included NOAA/VHRR (Very High Resolution Radiometer), GOES/VISSR (Visible Infrared Spin Scan Radiometer), and Landsat/MSS (Multispectral Scanner Subsystem). The characteristics of these sensor systems are described in that report.

The results of the analysis of the GOES imagery for the two episodes selected for analysis in this study are discussed below. In the earlier study, haze patterns could also be detected in the NOAA and Landsat images. The satellite images shown in the following discussion can be compared with the analysis of the SURE measurements presented in Section 3, and the meteorological conditions, discussed in Section 2.

4.1.1 Case 1: 19-23 July 1978

For each day of the July 1978 episode, three GOES visible channel images (mid-morning, early afternoon, and late afternoon) were examined. Of the three times of day, a haze pattern was best definable during the mid-morning hours. The imagery of the early and late afternoon hours displayed considerable low level, fair weather cumulus cloud cover over the area of elevated pollution levels. In most instances, this cloud contamination during times of maximum solar heating (afternoon) obscured any haze pattern that might otherwise have been detectable in the imagery.

In these GOES images, as well as in other satellite visible channel images, haze patterns associated with regional pollution episodes can be detected because of their increased level of scattering relative to the normal background brightness levels. This is particularly true when the haze pattern extends out over the usually darker background (without sun glint) of the ocean surface. Moreover, contrast between terrestrial features (such as between lakes and land areas) is reduced within the region of the haze patterns.

The haze patterns can be distinguished from clouds primarily because clouds are much brighter and tend to have more sharply defined edges.

Haze patterns, on the other hand, tend to display a generally higher brightness near the center of the area than at the outer periphery; thus, it is not always possible to define a distinct edge to the observed haze pattern. Concurrent thermal infrared imagery can be used to assess the existence of thin cirrus clouds. Even thin cirrus clouds, which may be transparent in the visible image, appear opaque in the thermal IR.

The GOES visible image (2 km resolution-sectorized) of 1330 GMT (0830 LST), 20 July 1978, is shown in Figure 4-1. This image displays small areas of haziness, as well as some cloudiness, near the western end of Lake Erie and northern Ohio and in central New York state. Each of these maximum brightness areas falls within the area of four miles or less visibility and within areas reporting average 24-hour sulfate levels of from 20 to 35 $\mu g/m^3$ (see Section 3).

The GOES visible image 24 hours later on 21 July, shown in Figure 4-2, displays considerably more haziness associated with the regional pollution episode. The band of maximum haze reflectance agrees well with the location of the southern half of the maximum 24-hour sulfate levels of from 30 to 40 $\mu g/m^3$. The area of the northern half of the band of maximum sulfate levels contains considerable cloud contamination at this time, severely restricting the detection of the more subtle high reflectance patterns associated with haziness. A boundary of lesser reflectance on this date falls generally between sulfate levels of from 10 to 20 $\mu g/m^3$.

By 1330 GMT on 22 July, the overall haze pattern is extremely well defined in the GOES image, as shown in Figure 4-3. The area of maximum reflectance, which extends from central Ohio eastward to well off the coast south of New England, corresponds closely with the area of minimum surface visibility in haze and the region of maximum 24-hour average sulfate levels of from 30 to 55 $\mu g/m^3$ for this date. The edge of the haze pattern in this image displays a distinct boundary at its eastern-most extent well off the coast over the darker ocean background, indicating a relatively sharp gradient in pollution levels.

On 23 July, the haze area observed in the 1330 GMT GOES image (Figure 4-4) displays a maximum reflectance extending eastward from the New Jersey and southern New England coastal region, well into the Atlantic. The western extent of this maximum reflectance area agrees well with the
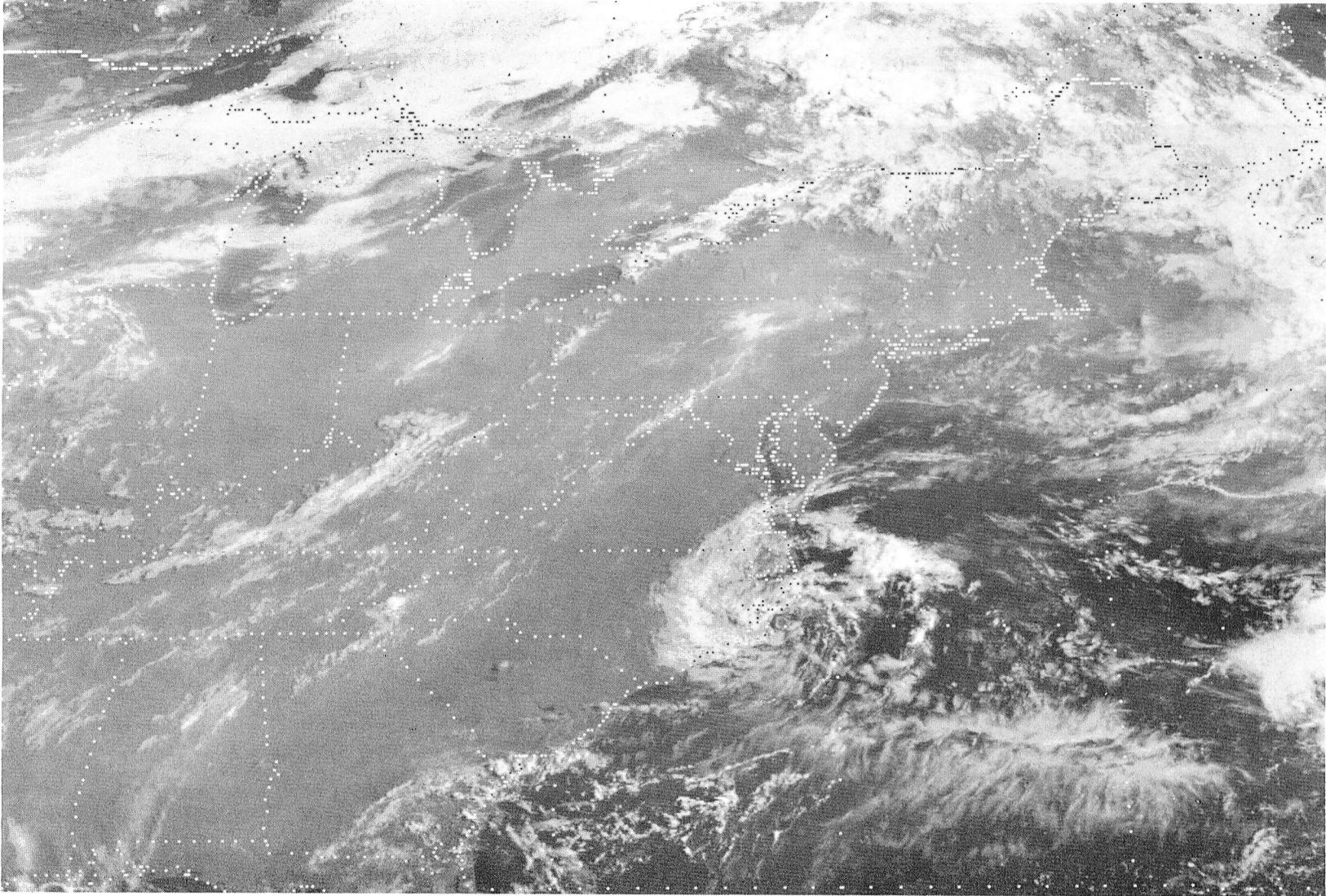
Figure 4-1   GOES Visible Image (2 km Resolution) at 1330 GMT, 20 July 1978
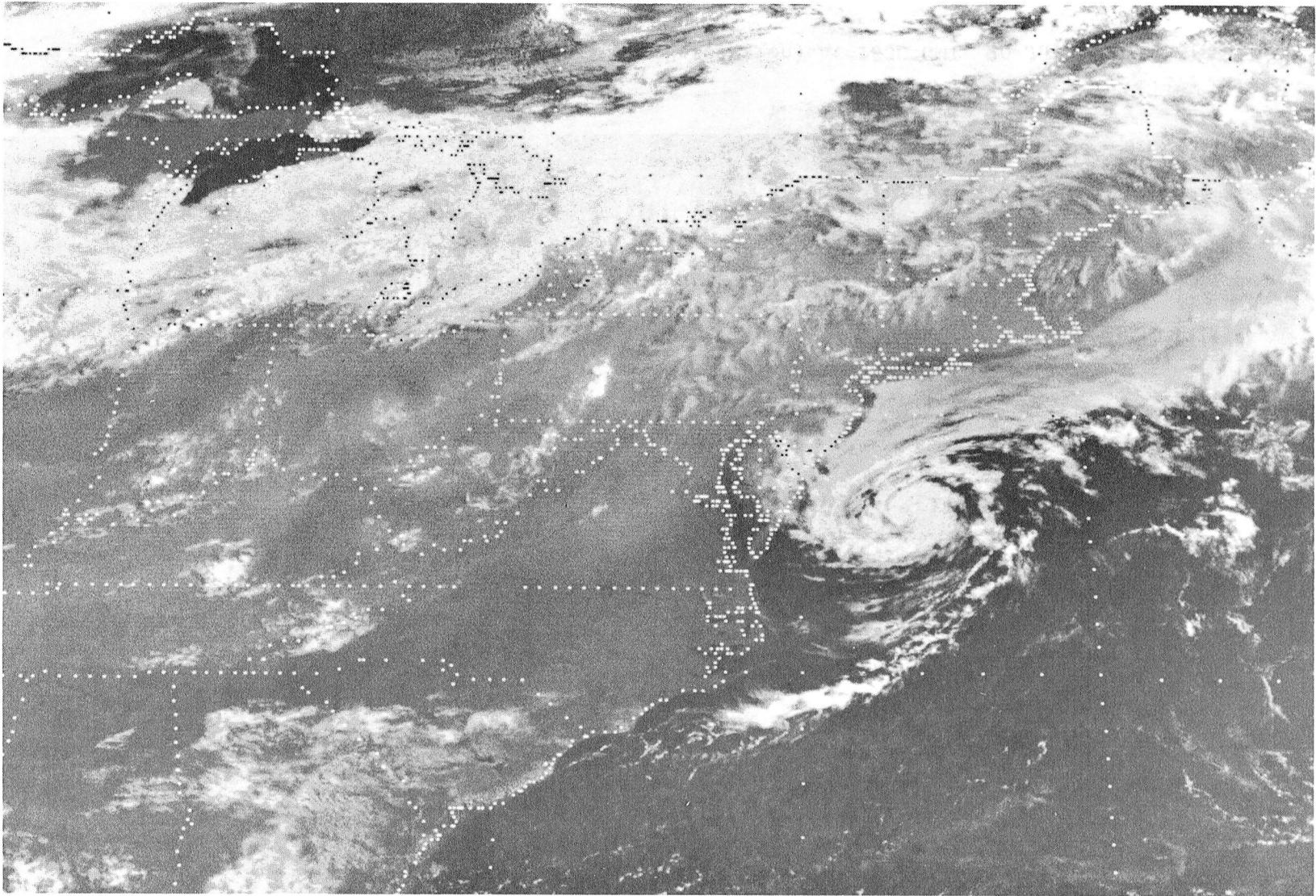
Figure 4-2   GOES Visible Image (2 km Resolution) at 1300 GMT, 21 July 1978
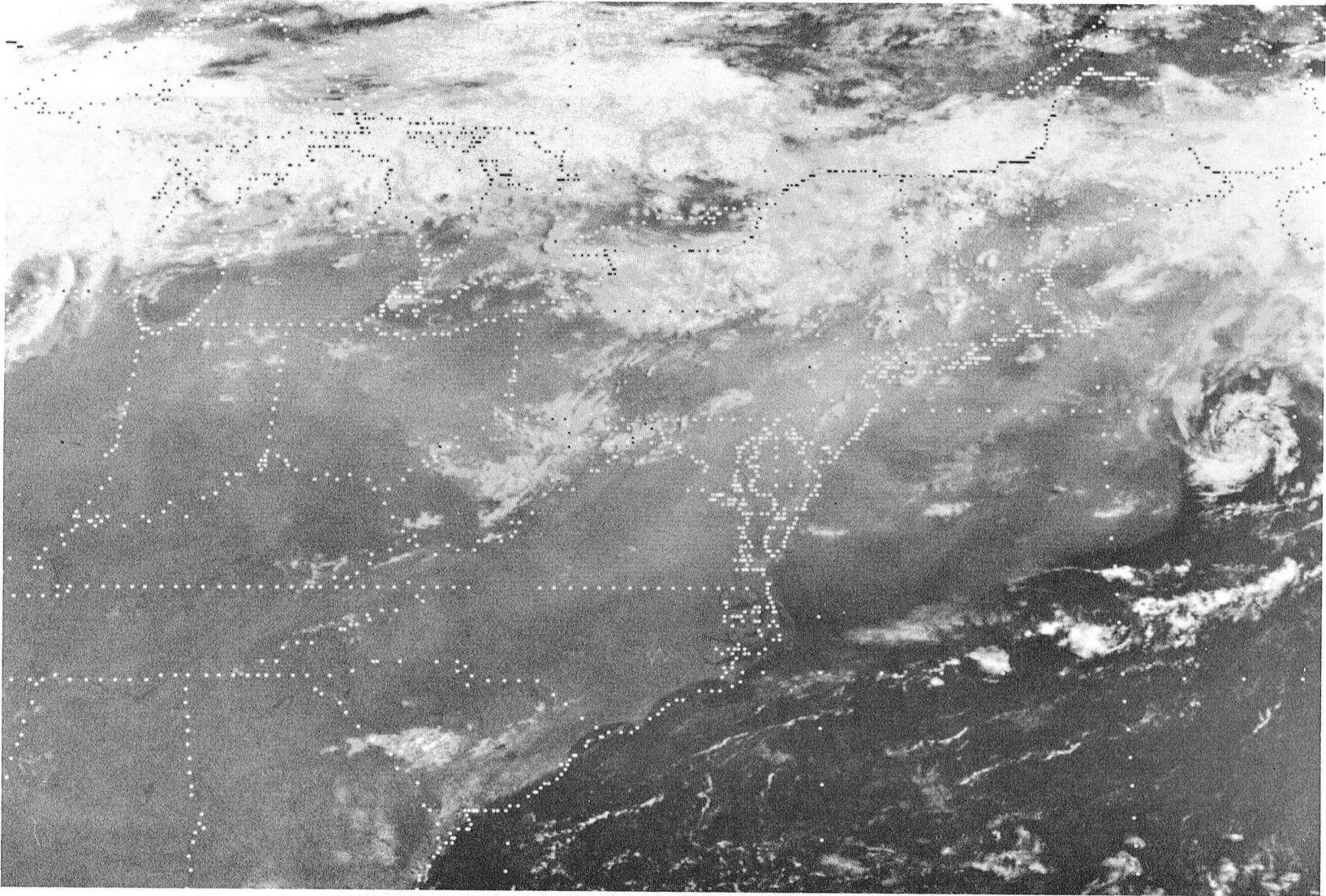
Figure 4-3 GOES Visible Image (2 km Resolution) at 1330 GMT, 22 July 1978
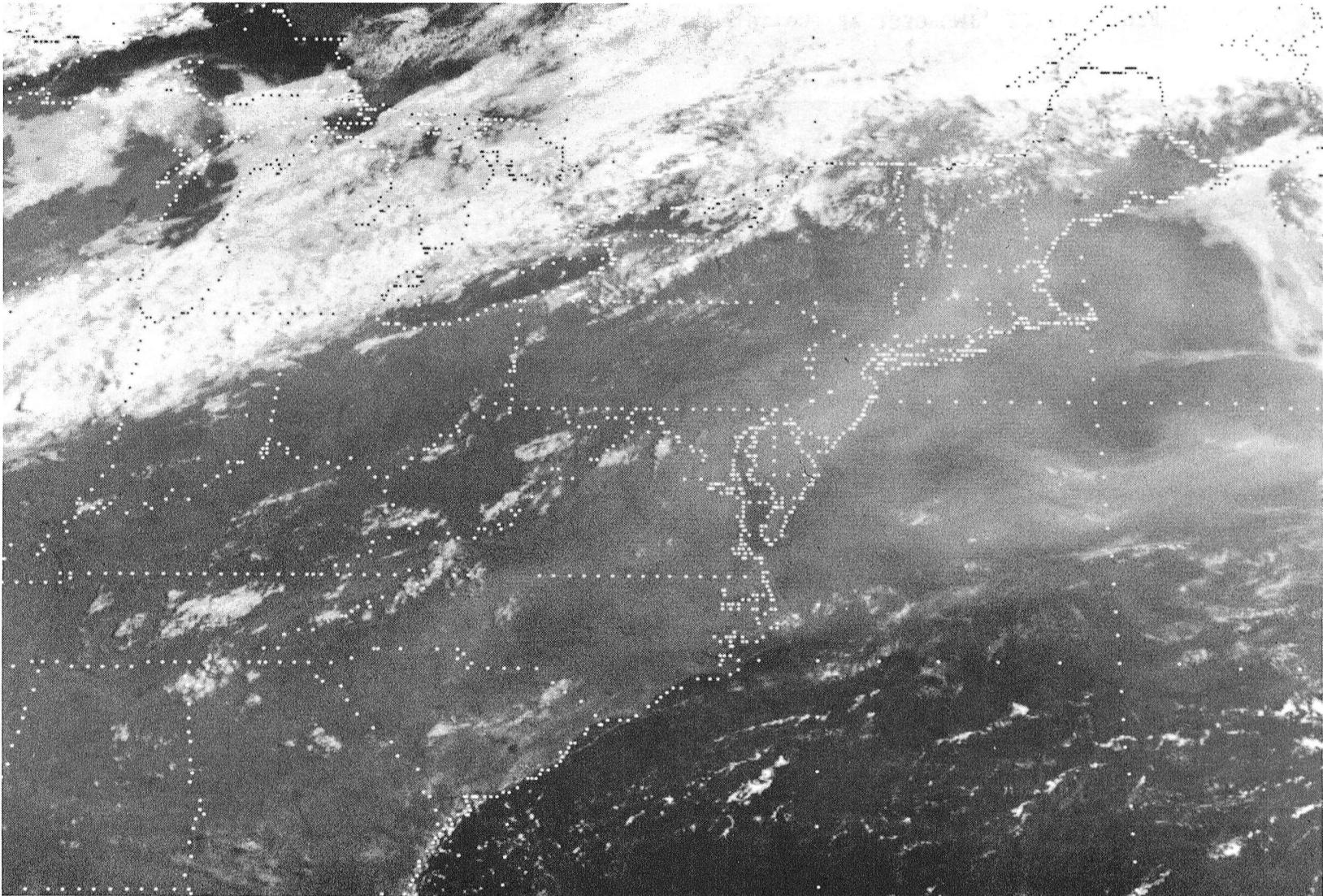
Figure 4-4   GOES Visible Image (2 km Resolution) at 1330 GMT, 23 July 1978

boundary of the >30 $\mu g/m^3$ sulfate level, and the area of minimum surface visibility. The boundary of the zone of lesser reflectance shows a generally good correlation to the western limit of the 20 $\mu g/m^3$ concentration.

4.1.2 Case 2: August 3-5, 1977

Analysis of NOAA and GOES satellite imagery for the period of 3-5 August indicated no well-defined haze patterns associated with the moderately high sulfate episode, as were evident in the July 1978 case. The early afternoon (1300 LST) GOES visible images (4 km resolution) for each of the three days are shown in Figures 4-5 through 4-7.

On 3 August (Figure 4-5), the initial day of increasing sulfate levels, highest concentrations are located over western Pennsylvania and eastern Ohio, immediately west of the weakening, stationary frontal system. Scattered to broken thin high clouds are observed over the region of maximum sulfate levels, and no haze area is in evidence.

By 4 August (Figure 4-6), sulfate levels have increased somewhat and advected slightly eastward into central Pennsylvania with readings >20 $\mu g/m^3$ extending as far east as central New England. Once again, however, there is no visible evidence of a haze area associated with the reduced surface visibilities. Scattered to broken low clouds (stratocumulus and cumulus) are observed over the region of highest sulfate concentrations. The bright cloud cells (cumulonimbus) located over southeastern Canada, are associated with a developing, weak cold front.

Considerably greater cloud amounts are in evidence by 5 August (Figure 4-7) as larger cumulus cloud clusters, associated with a weak cold front, are observed in eastern New York state and northeastern Vermont. Broken low level cloudiness is also present throughout the region of peak sulfate concentrations.

4.2 Effects of Cloud Cover on Detecting Haze

As previously stated, cloud contamination during times of maximum solar heating (afternoon) tended to obscure much of the haze pattern detectable in the early to mid-afternoon satellite imagery. This cloud build-up is, however, generally restricted to land areas where strong convection is taking place. Haze patterns extending eastward over the ocean areas are still detectable in the satellite imagery into the late
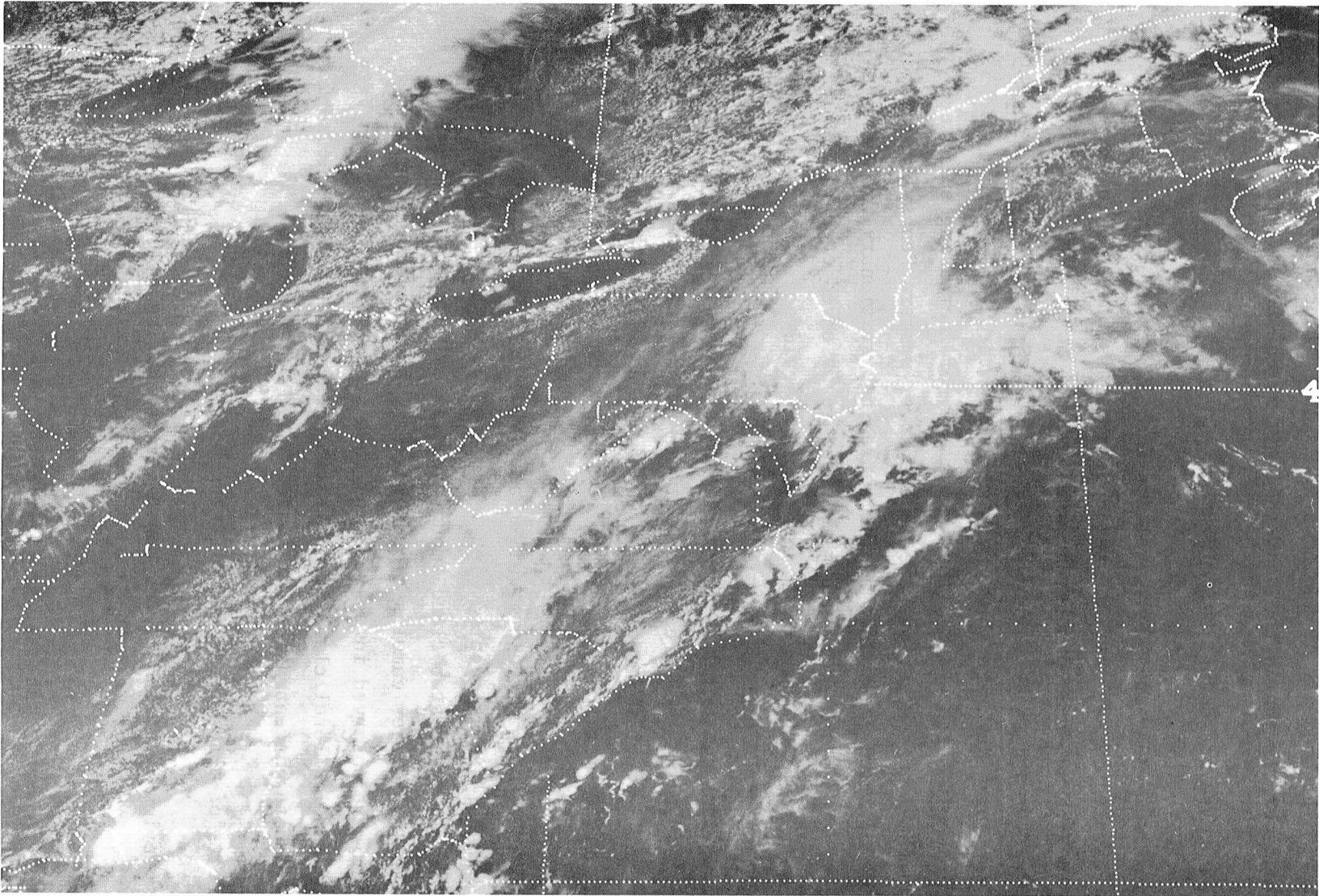
Figure 4-5   GOES Visible Image (4 km Resolution) at 1800 GMT, 3 August 1977
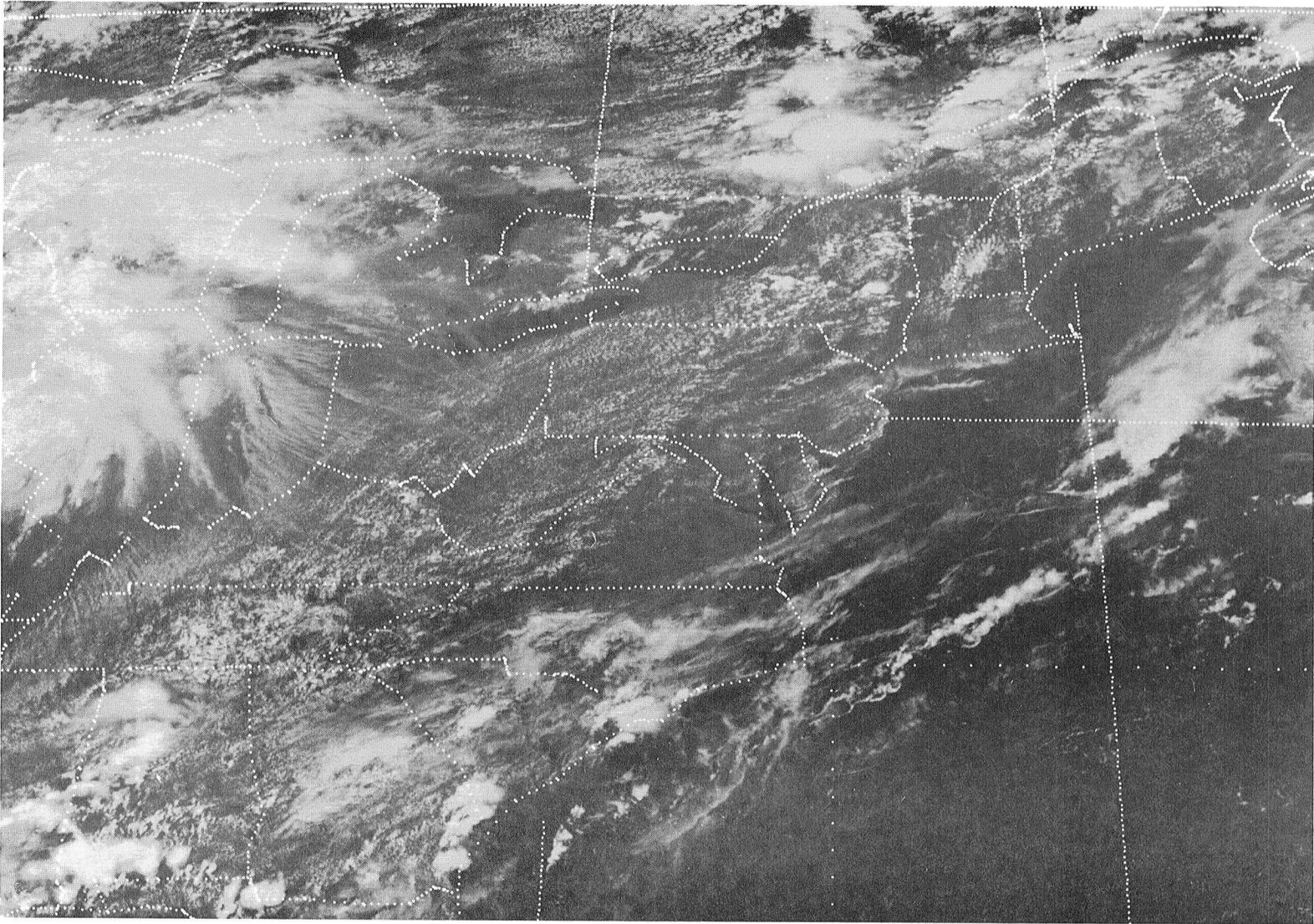
Figure 4-6   GOES Visible Image (4 km Resolution) at 1809 GMT, 4 August 1977
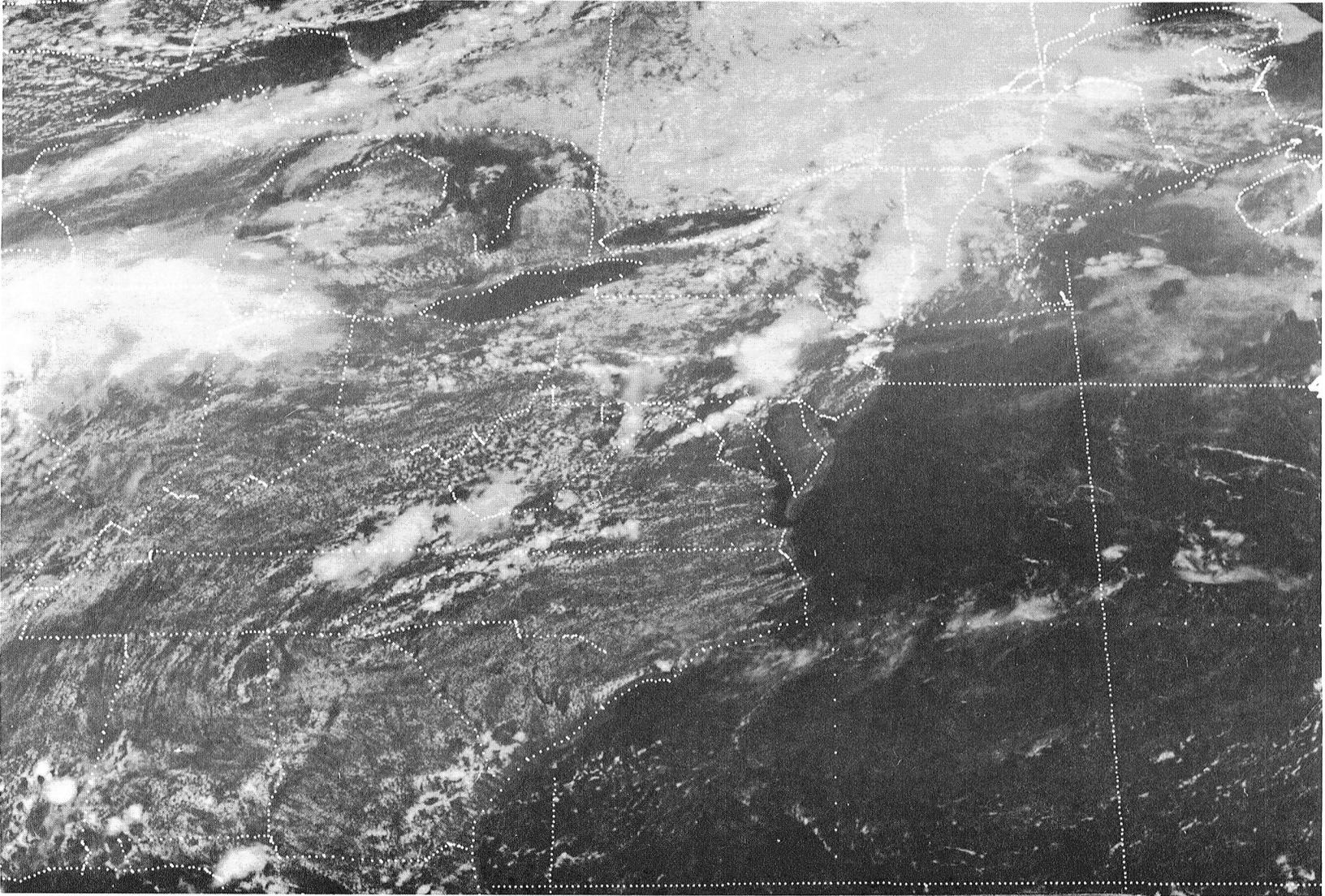
Figure 4-7   GOES Visible Image (4 km Resolution) at 1800 GMT, 5 August 1977

afternoon hours. The GOES visible image of 1730 GMT (1230 LST) on 22
July 1978 (Figure 4-8) already displays considerable buildup of low level,
convective clouds over the northeastern United States. Comparison with
the early morning GOES image (0830 LST) for this date, shown in Figure
4-3, reveals that much of the haze pattern previously observed over New
Jersey, Delaware, Maryland, eastern Pennsylvania and Virginia, is no
longer detectable. This is also true for the haze pattern displayed
earlier over portions of Ohio and Indiana. Note, however, that no low
level cloudiness is observed over the coastal waters, thus allowing the
haze pattern to remain well defined. Another example of early afternoon
cloud contamination is shown in Figure 4-9. Comparison with the early
morning GOES visible image (0830 LST) for 23 July 1978 (Figure 4-4)
reveals a similar low level, convective cloud build-up which obscures the
previously well defined haze pattern along the Northeast coastal region.
Again, however, the haze extent over the ocean region remains well defined
due to lack of convective cloud development.

The early afternoon GOES images for the August 1977 case (see Fig-
ures 4-5 through 4-7) showed that low cloudiness and fog were creating
problems for the possible detection of the haze area associated with the
high sulfate episode. The existence of a greater amount of cloudiness
during the period of that pollution episode may explain in part why the
haze pattern in the August 1977 case is not detectable as it is in the
July 1978 case.

4.3   Model Simulation of Regional Pollution Episodes from Space

4.3.1   Description of the Model

A computer program has been developed at ERT to simulate various
atmospheric conditions, including normal clear conditions and with clouds
or pollution layers, in both the visible and infrared spectral ranges.
The program consists of an atmospheric transmittance model (LOWTRAN 3B,
Selby et al, 1976) and a radiative transfer model (Burke and Sze, 1977)
with the capability of performing multiple scattering computations. The
input parameters include altitude profiles of atmospheric gaseous con-
stituents and temperature. In addition, the optical information of pol-
lution plumes and clouds can be inserted to the normal atmosphere to
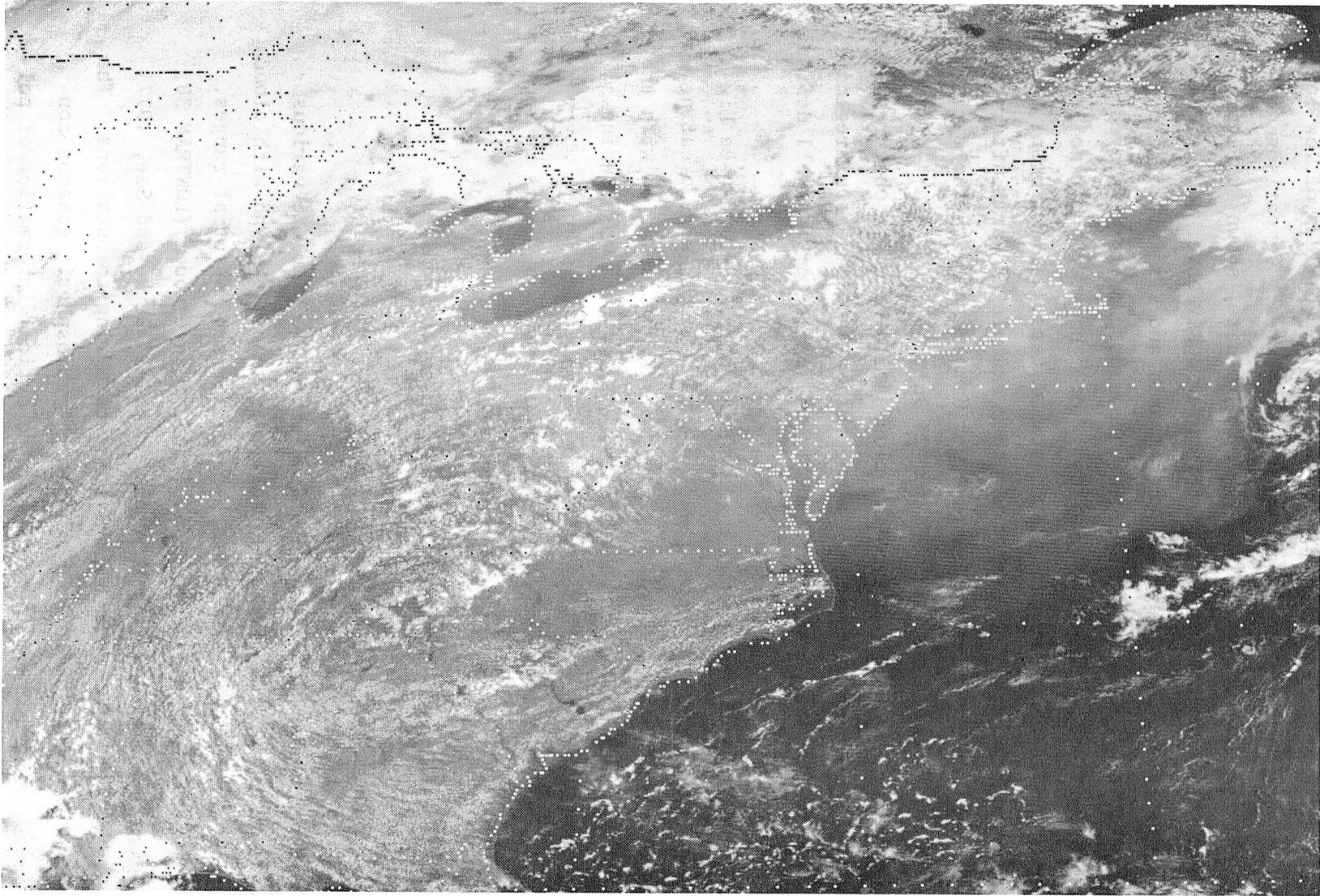
Figure 4-8   GOES Visible Image (2 km Resolution) at 1730 GMT, 22 July 1978
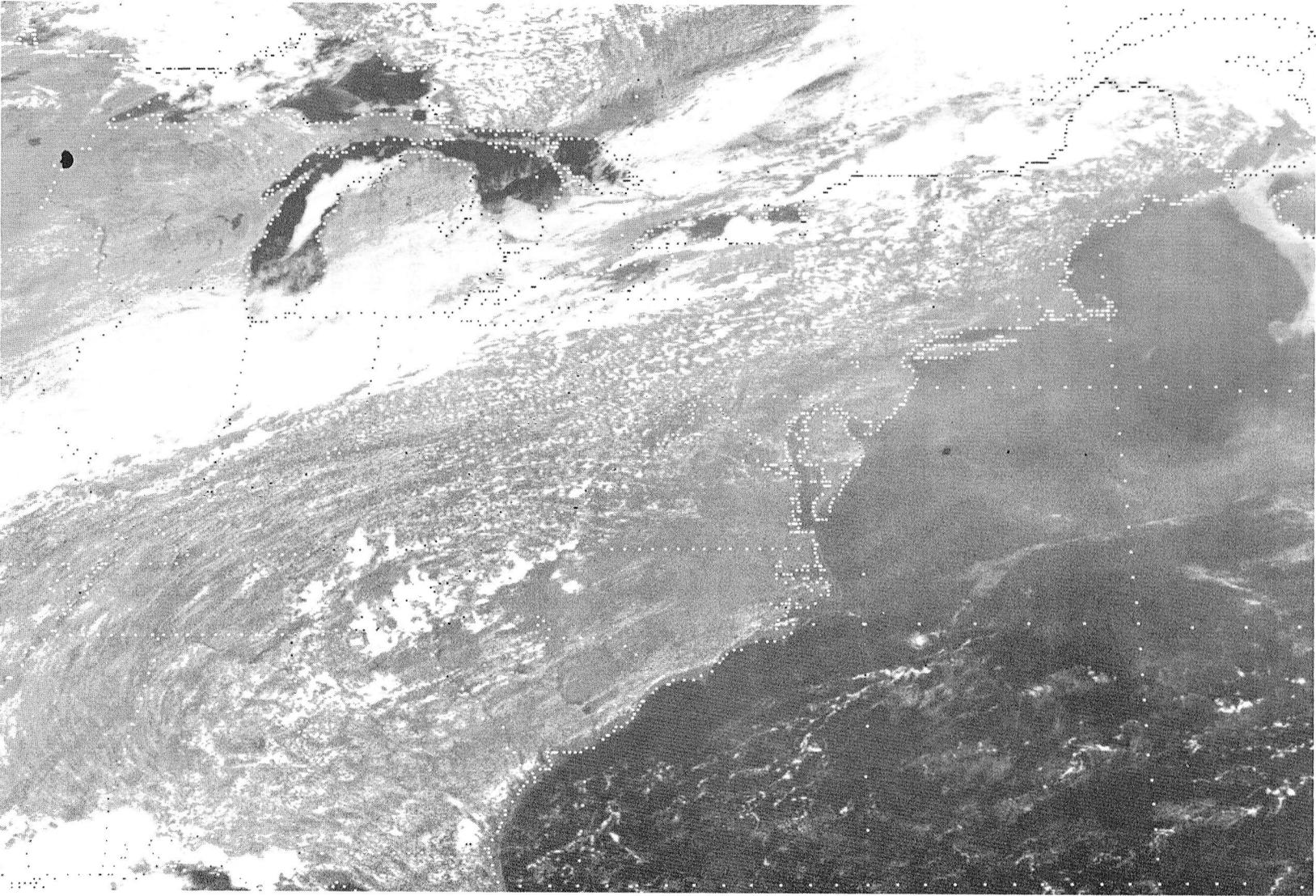
Figure 4-9   GOES Visible Image (2 km Resolution) at 1730 GMT, 23 July 1978

describe various atmospheric conditions. The output of the combined model can be intensity at any altitude (for satellite, airborne or ground measurements) for any sensor look angle (normal or slant). Some other applications of the model include the flux information for regional or global heat budget consideration and the integrated intensity at all levels for possible rate changes of atmospheric chemical reactions. A more detailed description of the model is given in Barnes et al (1979).

As the energy needs have been expanding during the past decade, emissions of sulfuric oxides (SO_x) and nitrogen oxides (NO_x) from power plants have also increased significantly. These gases oxidize to form sulfate (SO_4^{--}) and nitrate (NO_3^{-}), which (especially the sulfate) degrade the visibility. Although sulfate contributes only part of the total mass of pollutants, they have strong optical effects (the light scattering property). This effect is mainly due to their size range, which is only a few tenths of microns. Because these particles are the most effective light scatterers, it is feasible to detect and monitor from a space-borne sensor (or sensors) the pollution episodes with high sulfate concentrations. The other optical contributors include the suspended particulates and nitrogen dioxide. Defining the concentration and the size distribution of various pollutants, however, is yet another complex task for modeling as it depends upon wind speeds, relative humidity, mixing heights and other meteorological conditions (the model adopted for this study is the more frequently used Labadie plume size distribution).

A series of intensity computations have been carried out with various amounts of particulate masses. The pollution episodes analyzed in this study are all in the mid-west and northeast regions during summer months. Therefore, a standard mid-latitude summer atmosphere with a visibility of 23 km is assumed to be the unpolluted background conditions. The procedure used in these model computations can be summarized as follows:

(1) select an atmospheric model including prescribed temperature, humidity and gas constituent profiles, background visibility and surface reflectivity;

(2) define the solar angle and the satellite view angle;

(3) compute the atmospheric opacity and single scattering

profiles at defined wavelength;

(4) perform the radiative transfer computation for intensity as observed from satellite;

(5) introduce additional amounts of sulfate and suspended particulates representative of the regional concentrations and define the mixing height;

(6) repeat (3) and (4) to obtain the new intensity and thus the brightness contrast; and

(7) repeat (5) and (6) for different concentrations.

Results show that near dusk or dawn, when sunlight reaches the earth's surface in a slant path (away from normal), the contrast is more pronounced. For example, with a solar angle of 60° from the vertical, the nadir-viewing (vertically downward) intensity is close to 50% higher for a 50 $\mu g/m^3$ loading of sulfate than for clear conditions (no pollution). The contrast is reduced to less than 40% for the same case when the sun is overhead. Furthermore, the view angle also plays a role on the intensity. For example, if the sensor scans from 0° to 37° from the vertical, the relative brightness increases as the optical path increases when moving away from the vertical. The correction at the edge of the scan (37° from the vertical) is in the order of 10%.

4.3.2 Specific Atmospheric Parameters Required for Modeling

Some important parameters other than the standard atmospheric conditions for interpreting satellite information from the radiative transfer model include the surface reflectance and the mixing height. Reflectance is a function of the nature of the surface and the observation wavelength (Figure 4-10). In the visible range, both water and land (with the exception of certain types of sand, snow and ice) have low surface reflectances (0.2). In the near-infrared, the surface reflectance for water bodies is near zero but those for vegetation and soil increase rapidly up to 0.6. In the thermal infrared spectral range, all surfaces become near perfect emitters and the reflecting effect is negligible.

The mixing height is the height where the concentration of pollutant particles remains, in general, nearly constant from the surface to
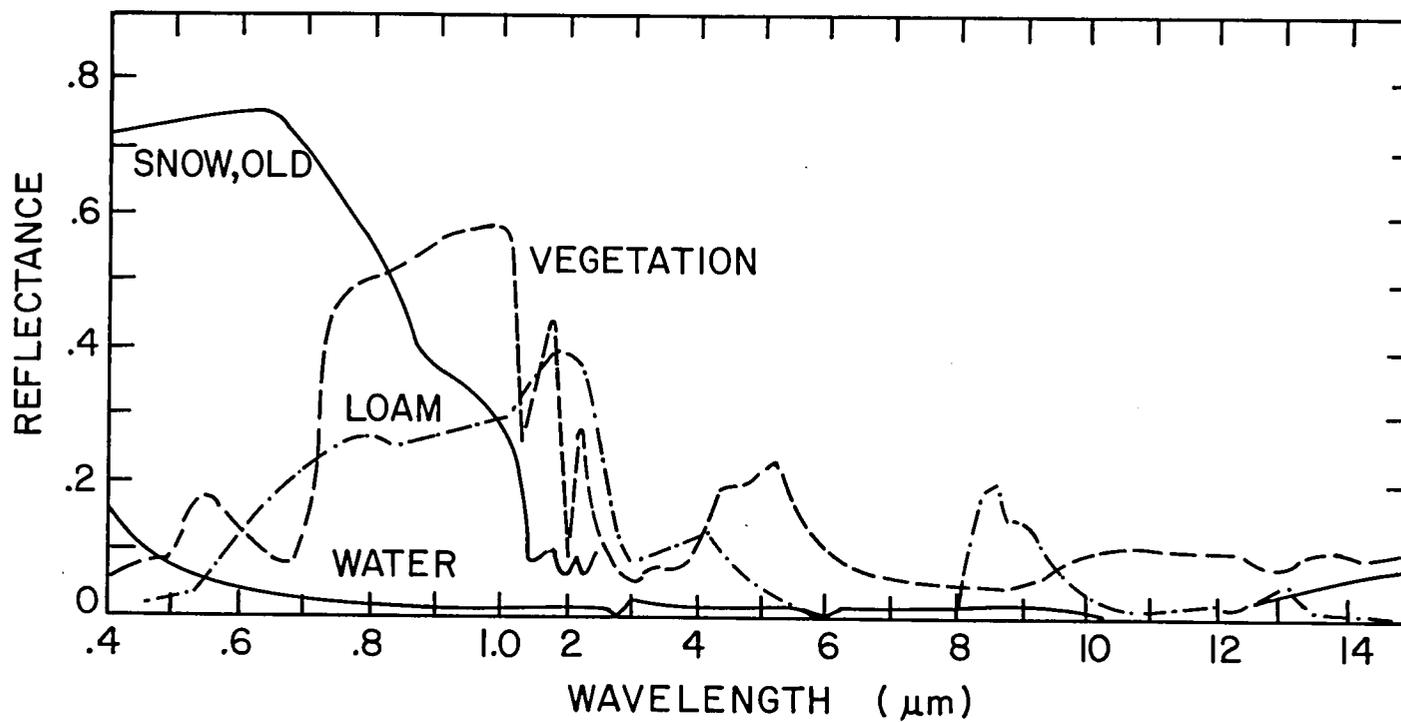
Figure 4-10   Typical Surface Reflectance of Water, Snow, Dry Soil and Vegetation (McClatchey et al, 1972)

that level and becomes substantially less beyond that level. This level is assumed to coincide with the meteorological "inversion height" which is defined as the level where the departure from the usual decrease of atmospheric temperature with altitude occurs. Such information can be obtained from the conventional temperature sounding. The knowledge of the mixing height is essential in order to retrieve surface concentration from satellite sensors. Without such information, only the total particulate amount (an integrated value of altitude) can be obtained.

4.4 Comparison of Model Results with Satellite Digitized Data

In the study by Barnes et al (1979) the model results for the July 1978 episode were compared with the satellite digitized data. Portions of the NOAA (visible range) digitized data for 21-22 July were processed and analyzed. Due to the excess amount of data, only certain scan lines were chosen for analysis. The brightness values from the satellite readout are on a linear scale from 0 to 255, with the lower numbers representing brighter values.

Figures 4-13 and 4-14 show some typical scan lines. The values of brightness (relatively intensity) have been subtracted from 255 in the original data set such that higher numbers represent brighter or higher intensity values. Each scan line consists of 2000 pixels. Figure 4-11 shows that between pixels 150 and 350, around 500, and between 1600 and 2000, substantial cloudiness existed, giving rise to the sporadic high brightness readings against the background. A relative maximum occurred between pixels 600 and 750, where the relative intensity value is close to 55, against a typical background value of 35. Similar patterns are also observed in another scan line (Figure 4-12), which was about 50 km south of the previous scan line.

In the analysis, distinguishing between clouds and haze areas is relatively simple since clouds exhibit a much higher reflectance (brightness) than do hazes. Furthermore, the gradient in brightness associated with cloud edges is quite distinct at the NOAA resolution of 1 km, whereas for the polluted regions, the change in brightness is much less sharp.

The scan lines, shown in Figures 4-13 and 4-14, cover the heavily polluted regions and also areas where unpolluted background values are represented. The satellite readout times were 1520 and 1536 GMT on 21

43
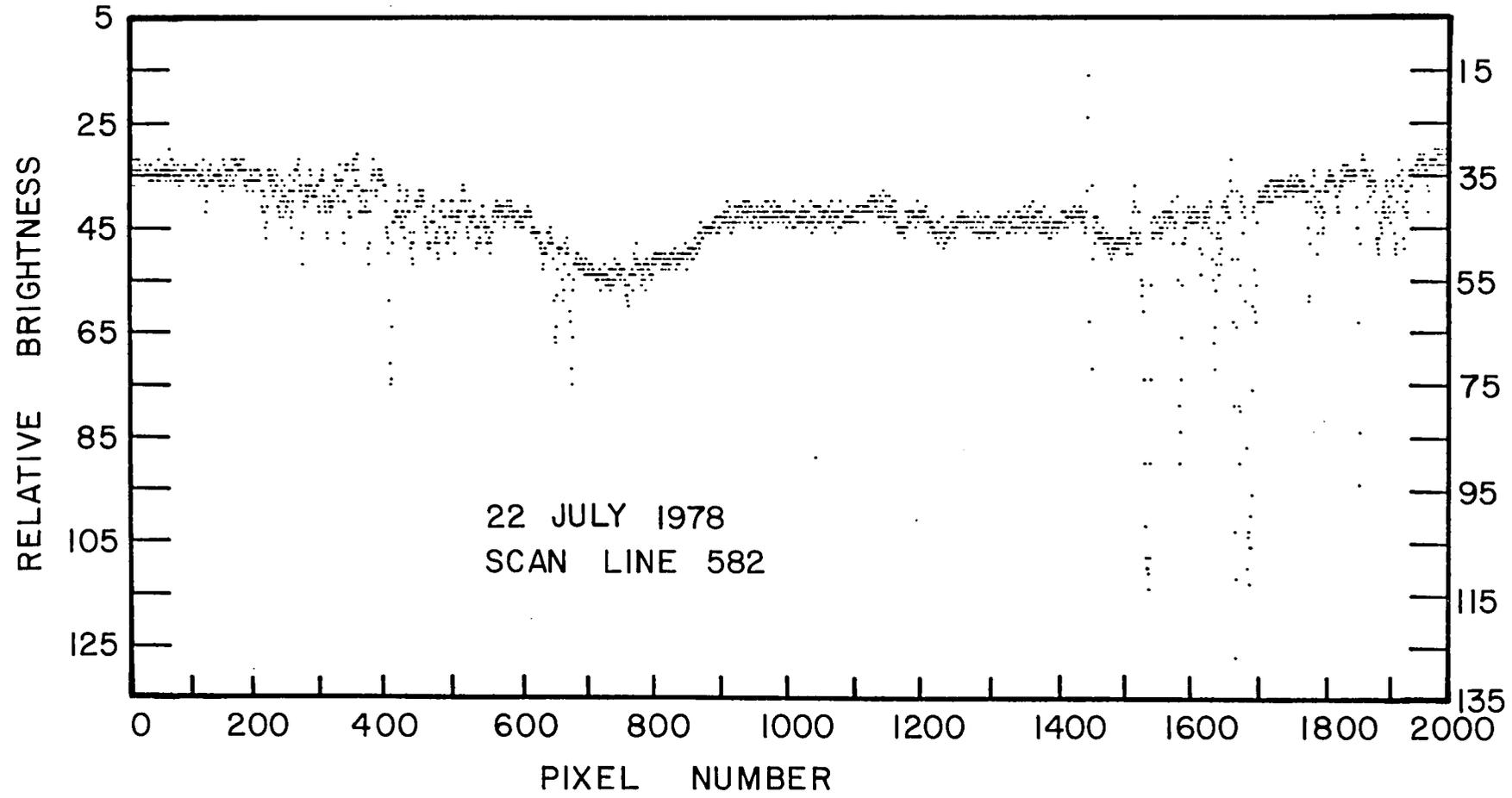
Figure 4-11   Digital Data Display from a Typical NOAA/VHRR Scan Line, which Consists of 2000 Pixels. The Location of the Scan Line is Shown in Figure 4-14 (Second Line from the Top). Average Values were Taken for Every Hundred Pixels

44
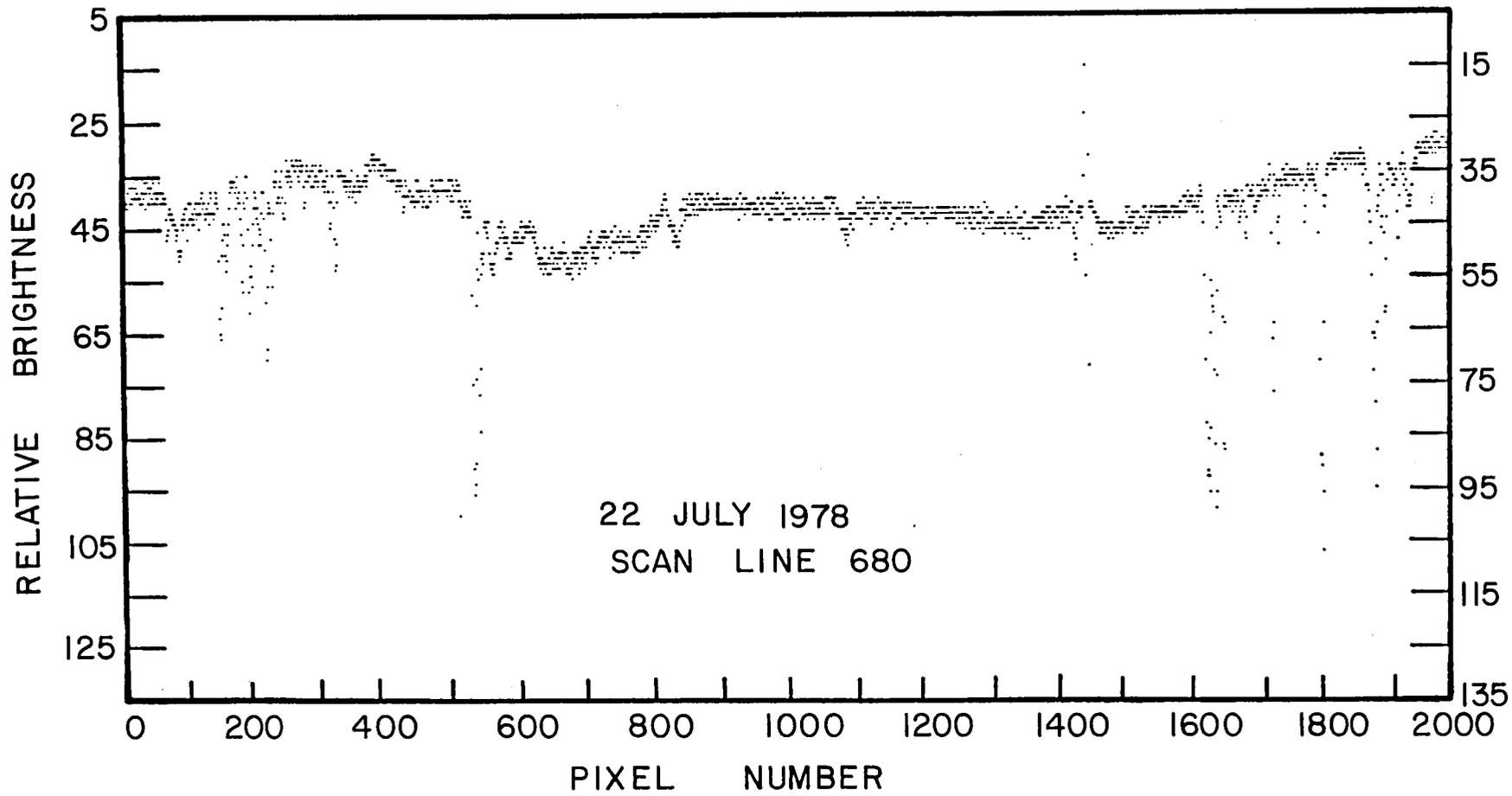
Figure 4-12   Digital Data Display from Scan Line, which Corresponds to the Third Line from the Top on the Right in Figure 4-14
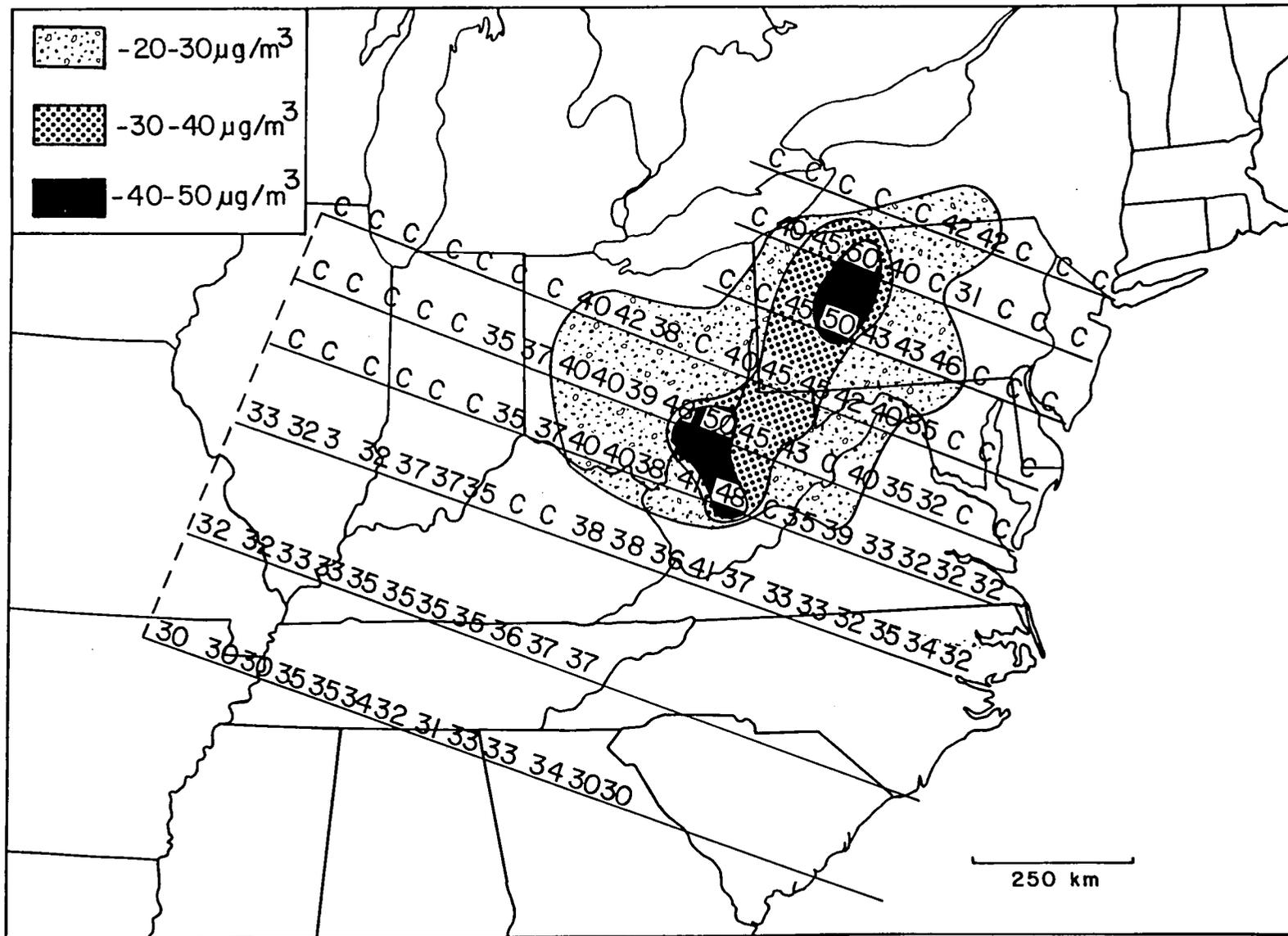
Figure 4-13   Relative Brightness Along Scan Lines Chosen for July 21, 1978 and Estimated Sulfate Concentration by Model Calculation

Figure 4-14   Relative Brightness Along Scan Lines Chosen for July 22, 1978 and Estimated Sulfate Concentration by Model Calculation

and 22 July, which correspond to 1020 and 1036 local standard times. The sun angles were about 30° from normal.

The brightness values were averaged for every hundred pixels, as shown in Figures 4-13 and 4-14. The designator "C" represents regions of substantial cloud coverage. The brightness ratios are obtained and compared with model results to create a synoptic map of sulfate concentrations. Sulfate concentrations in the dark, medium, and light-toned regions are estimated as 40-50, 30-40 and 20-30 $\mu g/m^3$, respectively. The high concentrations of 21 July were largely in the eastern part of Ohio, extending into western Pennsylvania and northern West Virginia. On 22 July, the haze area had moved eastward into the southeast Pennsylvania and New Jersey area. The areas of pronounced concentrations were approximately 500 km x 500 km on 21 July and 250 km x 500 km (over land only) on 22 July.

The results, both in terms of concentration and areal extent, generally agree with the 24-hour average synoptic maps produced by the SURE ground measurements of both Class I and Class II stations (Figures 3-3 and 3-4). Furthermore, they can be compared to the 3-hour average (0900 to 1200 hours) sulfate values at the nine Class I stations (Figures 4-15 and 4-16). Due to the spatial spread of the Class I stations, synoptic maps can not be derived for the 3-hour averages. However, the transition of the polluted area from the mid-west region to the east is clearly shown. For example, at Fort Wayne, Indiana and Rockport, Kentucky, average sulfate values for 0900 to 1200 hours on 21 July were 31.7 and 15.4 $\mu g/m^3$, respectively. For the same time period on 22 July, the values have dropped to 27.3 and 2.5 $\mu g/m^3$ for the respective stations. Another distinctive example is the Indian River, Delaware reporting station; from 21 July to 22 July, the average value of sulfate between 0900 and 1200 hours increased drastically from 7.2 to 40.9 $\mu g/m^3$.

One problem is that in the analysis some hazy areas were obscured by clouds and therefore could not be detected from satellite sensors. For example, at Montague, Massachusetts, the sulfate readings were high on both 21 July and 22 July (31.2 and 44.0 $\mu g/m^3$, respectively, for the same time period); a haze pattern could not be detected in the satellite imagery for this area, however, because of extensive cloud cover.
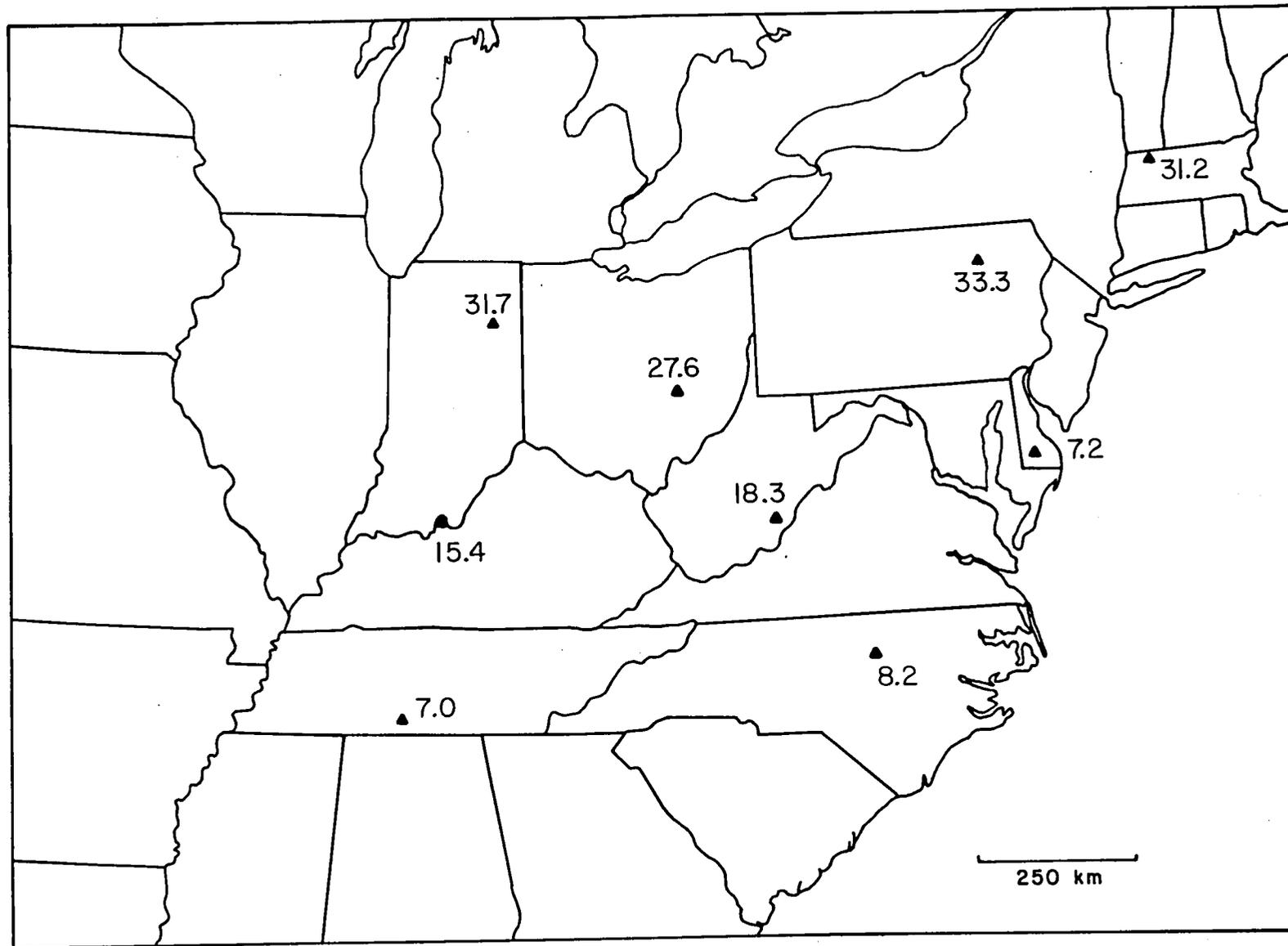
Figure 4-15   Average Sulfate Concentrations ($\mu g/m^3$) between 1900 and 1200 Hours, 21 July 1978 Taken from Nine Class I SURE Stations
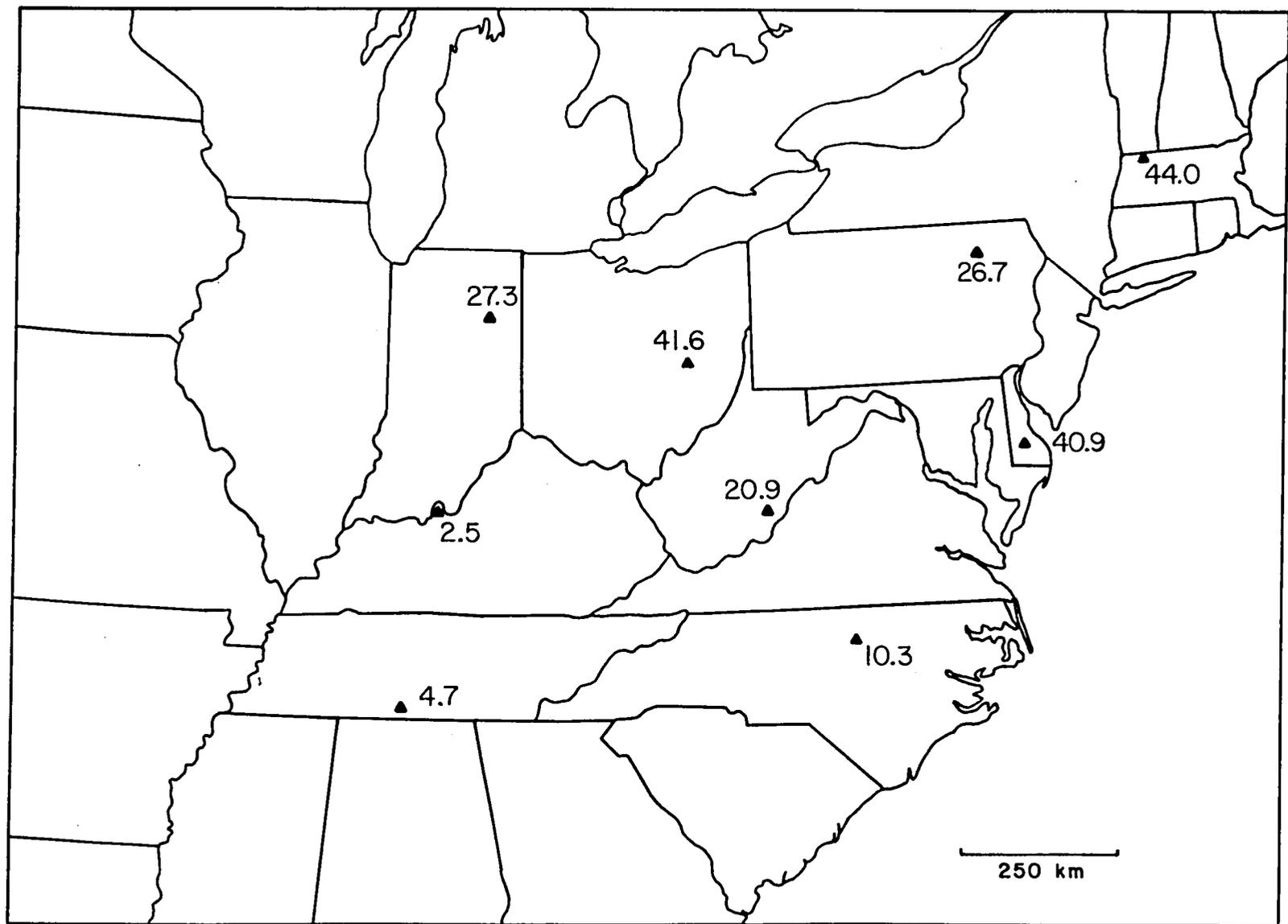
Figure 4-16   Average Sulfate Concentrations ($\mu g/m^3$) between 0900 and 1200 Hours, 22 July 1978 Taken from Nine Class I SURE Stations

5. EVALUATION OF REQUIRED PARAMETERS FOR MAPPING REGIONAL POLLUTION EPISODES

5.1 Summary of Characteristics of Pollution Episodes

The two cases analyzed were summertime haze episodes, in which sulfates are an important constituent although other particulates are also present. In each case, both 24-hour and 3-hour sulfate levels greater than 20 $\mu g/m^3$ were measured on each day of the episode. The characteristics of the two episodes, as defined by the SURE data base, can be summarized as follows:

(a) the durations of the two episodes were three and five days, respectively; the episodes were multi-day, but each lasted less than a week. The sulfate levels were observed to increase over the duration of the episode, so that the longer the duration of the pollution episode, the higher the sulfate levels;

(b) the sulfate levels ranged from 24-hour average values of 20 $\mu g/m^3$ to more than 50 $\mu g/m^3$, with considerable diurnal variation. For the July 1978 case, the peak levels occurred generally between local noon and 1500 LST, whereas minimum levels occurred between 0300 and 0600 LST. Diurnal variations of as much as 10 to 20 $\mu g/m^3$ were observed at many stations; in one instance, an increase of 60 $\mu g/m^3$ over a six-hour period was observed;

(c) in the two cases studied, the area covered by sulfate levels exceeding 20 $\mu g/m^3$ was observed to be as much as 1500 km long by 500 km wide. The area of critical sulfate levels (>20 $\mu g/m^3$) was considerably smaller in the early morning hours than at the time of peak levels, in the early afternoon;

(d) the spatial gradients of 24-hour average sulfate levels were generally small, but were observed to reach steeper values (as much as 20 $\mu g/m^3$ over a distance of 75 km) in certain locations; and

(e) the characteristic meteorological conditions for both
     cases were stagnant high pressure systems covering the
     eastern United States, bringing in warm, humid tropical
     maritime air (daytime temperatures exceeding 30°C and
     dewpoints exceeding 20°C) with southerly wind flow. The
     areas of maximum sulfate levels were transported east-
     ward throughout each episode.

5.2 Ranking of Parameters Required for Episode Mapping

5.2.1 Parameters Based on Analysis of SURE Data

Based on the characteristics of the two episodes, as derived from
the SURE data, the key considerations required for episode mapping from
satellite sensors are the following:

(a) detection of sulfate levels exceeding 20 $\mu g/m^3$;

(b) capability to view a broad area (of the order of 1500 km
     swath) because of regional extent of pollution episodes;

(c) spatial resolution sufficient to detect variations in
     sulfate levels of greater than 10 $\mu g/m^3$ over distances
     of the order of 50 to 75 km;

(d) repeat coverage at least on a daily basis; and

(e) at least one of the daily observations should be during
     the mid to late morning local time, when the sulfate
     levels have begun to increase after the early morning
     minimum levels, and convective-type cloud cover has not
     yet increased to the amount reached later in the after-
     noon.

5.2.2 Additional Parameters Based on Spectral Analysis

The Wavelength Requirement

Data from only the visual wavelength sensors were fully analyzed in
this study. In the near infrared range, the atmosphere is more trans-
parent and therefore in theory should be more sensitive to the existence

of pollutants. However, it is also shown in Figure 4-10 that in the near-infrared range, the land surfaces have higher reflectance values with greater variabilities. Such an effect may offset the advantage of the near-infrared sensors for detection of hazy areas over land. On the other hand, near-infrared sensors are a very useful tool to detect haze patterns over water bodies. Furthermore, a near-infrared band at 1.4 or 1.7 µm is very sensitive to the existence of atmospheric water vapor. Therefore, a combined visible and near-infrared sensor system would be desirable to delineate aerosol haze regions from water vapor haze regions.

In the window region (10 to 12 µm) of the thermal infrared range, the atmosphere is relatively transparent and therefore, a sensor in that range would be useful for haze detection. It has also the advantage over visible and near-infrared sensors that it can be used at nighttime. The only disadvantage is that aerosols are less effective scatterers in the thermal infrared range and maximum sensitivity cannot be obtained. A thermal infrared sensor can provide nighttime observations for deriving information on the diurnal variation of an episode that lasts over a few days.

In essence, a combined visible, near-infrared and thermal infrared sensor system is the most desirable for monitoring regional pollution episodes. The visible and near-infrared sensors provide information of the particulate amount during the day over various surface backgrounds. The thermal infrared sensor provides additional nighttime information throughout the growth and dissipation phases of the episode.

The Bandwidth Requirement

The currently available satellite sensors provide information on the amount of the total particulate mass utilizing atmospheric radiative transfer models. With additional assumptions, this information can then be converted to provide an estimate of the surface sulfate concentrations. Since there are strong absorption lines for both sulfate and acid sulfate particles in the infrared spectral range, direct observations of such species at those wavelengths would thus be more desirable. Recent investigations indicate that there are strong bands at 9.0 µm and 16.1 µm for sulfate particles (Cunningham et al, 1974) and at 8.3 µm, 9.4 µm, 11.5 µm and 16.7 µm for acid sulfates (Cunningham and Johnson, 1976).

These are all very narrow bands with bandwidth in the order of 0.25 μm.
Current satellite infrared sensors, on the other hand, all respond to a
fairly wide spectral range. For example, both GOES and Landsat infrared
sensors operate in the 10.5 to 12.5 μm wavelength range. With such a
wide spectral response, the distinct sulfate or acid sulfate absorption
features are not likely to be observed. Therefore, narrow band infrared
sensors will have to be used in order to obtain specific information of
atmospheric sulfate particles.

6. CONCLUSIONS

6.1 Evaluation of Existing Sensor Systems for Monitoring Regional Pollution Episodes

In the study by Barnes et al (1979), data were examined from three satellite systems: GOES, NOAA and Landsat. In accordance with the parameters listed in Section 5, a cursory evaluation can be made of each of these sensor systems for monitoring regional pollution episodes.

6.1.1 GOES/VISSR

Many of the requirements for mapping regional pollution episodes are satisfied by the GOES sensor system. The GOES provides observations every day, so it satisfies the temporal measurement requirements. In fact, the GOES capability of viewing a region nearly continuously (every half-hour) increases the chances of obtaining a cloud-free observation, as well as providing opportunities for observations at various sun angles including low angles in early morning and late afternoon. The area viewed by GOES is extensive (full earth's disc) and the spatial resolution (4 km or better) is more than adequate. The GOES radiometer has only visible and thermal infrared channels, so is affected by clouds. Moreover, the results of the analysis in the earlier study indicated that haze patterns in some relatively cloud-free cases could not be detected in the visible-channel imagery even though sulfate levels exceeding 20 $\mu g/m^3$ were reported.

6.1.2 NOAA/VHRR

The NOAA/VHRR also satisfies many of the mapping requirements. Since this system is a polar-orbiting satellite, the observations are limited to one daytime and one nighttime pass, thus restricting the temporal coverage. Although the area viewed is not as extensive as with GOES, the data swath is sufficient for viewing regional-scale patterns. The spatial resolution of the VHRR (1 km) is more than adequate. As with the GOES, the VHRR is a two-channel sensor (visible and thermal infrared), hence, the same problems of cloud interference, and haze patterns not always being detectable unless the episode has built-up over several days, are experienced.

6.1.3 Landsat/MSS

A remote sensing system with the characteristics of Landsat is not useful for monitoring regional pollution episodes. The repeat coverage of once every 18 days (nine days if two spacecraft are in orbit) does not satisfy the temporal measurement requirements, and the viewing swath of only 185 km is completely inadequate for the required spatial coverage. The Landsat Multispectral Scanner (MSS) is also limited by clouds, although the multispectral capability of the sensor does offer some advantage over the broad spectral bands (visible) of the GOES/VISSR and NOAA/VHRR.

6.2 Considerations for Optimum Sensor System for Monitoring Regional Pollution Episodes

The data sample examined in the study was limited to two pollution episode cases. Nevertheless, the SURE data base has provided for the first time sulfate measurements from a regional network, making possible an analysis of the temporal and spatial characteristics of critical pollution episodes on a regional scale. Based on the results of the analysis, it is possible to evaluate the temporal and spatial resolution requirements of remote sensing systems for monitoring regional pollution episodes. It must be recognized that the evaluation is based on the measurements made during summertime haze episodes, of which sulfates are a major constituent; no attempt has been made to distinguish the different aerosol components which make up the haze episode.

Based on the results of the analysis, the general conclusions regarding an optimum remote sensing system for monitoring regional pollution episodes are as follows:

(a) the repeat coverage should be at least that of a polar-orbiting, NOAA-type satellite (twice-per-day coverage). The availability of an observation every half-hour as is possible from GOES, provides greater flexibility with regard to obtaining cloud-free observations; however, observations at one-half hour intervals throughout the day would generally not be required;

(b) an area viewed as large as that possible with GOES is not necessarily required. For a polar-orbiting satellite, however, a data swath at least as wide as that of the NOAA/VHRR (about 2000 km) is essential;

(c) the spatial resolutions of the NOAA and GOES sensors are more than adequate; in fact, a resolution of the order of 25 km may be sufficient for monitoring on a regional scale; and

(d) a pollution monitoring sensor system cannot depend on visible or thermal infrared channels, alone. Sensors limited to these spectral bands are restricted by clouds and may not detect a haze pattern in every instance when sulfate levels exceed the critical value of 20 $\mu g/m^3$. Furthermore, theoretical studies have indicated that a narrow band in the near-infrared as an additional channel may be useful for distinguishing sulfate from other aerosol components when clouds are not present.

The results of the analysis of satellite imagery and of computations using theoretical models, such as reported by Barnes et al (1979) have demonstrated the potential of utilizing remote sensing from satellites to monitor regional air pollution episodes. In the current study, the spatial and temporal measurement requirements have been examined more carefully using the unique SURE data base. The results of the evaluation of the considerations required for mapping pollution episodes provides information useful for the development of new observational systems to overcome the deficiencies of existing systems. For example, the optimum sensor system may be one in which high spatial resolution is sacrificed for greater sensitivity in detecting sulfates and other atmospheric aerosols and gasses. It is essential that efforts to develop improved remote sensing systems be continued to provide eventually a reliable, operational tool for monitoring critical air pollution episodes on a regional scale.

7. REFERENCES

Barnes, J.C., C.J. Bowley and H.K. Burke, 1979: Evaluation of the Capabilities of Satellite Imagery for Monitoring Regional Air Pollution Episodes, Final Report under Contract No. NAS1-15307 for NASA Langley Research Center, Environmental Research & Technology, Inc., Concord, MA (in publication).

Batchelder, R.B. and E.Y. Tong, 1978: Aerometric Data Compilation and Analysis for Regional Sulfate Modeling, Teknekron, Inc., Berkeley, CA.

Bowley, C.J., J.L. Horowitz and J.C. Barnes, 1977: Analysis of Photochemical Oxidant and Particulate Pollution in New England Using Remote Sensing Data, Final Report under Contract No. 68-02-2533 for EPA Region I Air Branch, Environmental Research & Technology, Inc., Concord, MA.

Brown, F.R. and F.S. Karn, 1976: Air Pollution from the Ohio River and Monongahela River Valleys, ERTS-1, A New Window on Our Planet, U.S. Geological Survey, Professional Paper 929, 261-265.

Cunningham, P.T., S.A. Johnson and R.T. Yang, 1974: Variations in Chemistry of Airborne Particulate Material with Particle Size and Time, Env. Sci. Tech., 8, 131.

Cunningham, P.T. and S.A. Johnson, 1976: Spectroscopic Observation of Acid Sulfate in Atmospheric Particulate Samples, Science, 191, 77.

Environmental Protection Agency, 1974: Health Consequences of Sulfur Oxides: A Report from CHESS 1970-1971, EPA-650/1-74-004, Human Studies Laboratory, National Environmental Research Center, Research Triangle Park, NC.

Environmental Protection Agency, 1975: Position Paper on Regulation of Atmospheric Sulfate, Report No. EPA-450/2-75-007, Office of Air Quality Planning and Standards, Research Triangle Park, NC.

Fraser, R.S., 1976: Satellite Measurement of Mass of Sahara Dust in the Atmosphere, Applied Optics 15, 10, 2471-2479.

Griggs, M., 1973: A Method to Measure the Atmospheric Aerosol Content Using ERTS Data, Third ERTS Symposium, Paper E2, 1505-1518.

Griggs, M., 1978: Determination of Aerosol Content in the Atmosphere from Landsat Data, Final Report under Contract NAS5-20899 for NASA/ Goddard Space Flight Center, Science Applications, Inc., La Jolla, CA.

Hidy, G.M., et al, 1977: Preliminary Air Quality Analysis of Urban and Regional Sulfate Distributions, Report 4295, American Petroleum Institute, Washington, D.C.

REFERENCES (cont)

Husar, R.B., N.V. Gillani, J.D. Husar, C.C. Paley and P.N. Turcu, 1976: Long Range Transport of Pollutants Observed through Visibility Contour Maps, Weather Maps and Trajectory Analysis, Proc. Third Symposium on Atmospheric Turbulence, Diffusion and Air Quality, October 19-22, 1976, Raleigh, NC, American Meteor. Soc, 344-347.

Lyons, W.A. and R.A. Northouse, 1973: Use of ERTS-1 Imagery in Air Pollution and Mesometeorological Studies Around the Great Lakes, Third ERTS Symposium, Paper E1, 1491-1504.

Lyons, W.A. and R.B. Husar, 1976: SMS/GOES Visible Images Detect a Synoptic-Scale Air Pollution Episode, Monthly Weather Review, 104, 1623-1626.

McClatchey, R.A., R.W. Fenn, J.E.A. Selby, F.E. Volz and J.S. Garing, 1972: Optical Properties of the Atmosphere - 3rd Edition, AFCRL-72-0497.

McClellan, A., IV, 1971: Satellite Remote Sensing of Large-Scale Atmospheric Pollution, Proc. Second International Clean Air Congress, Academic Press, NY, p. 1408.

Mueller, P.K., et al, 1979: The Occurrence of Atmospheric Aerosols in the Northeastern United States, Paper presented at the Conference of Aerosols: Anthropogenic and Natural Sources and Transport, New York Academy of Sciences, New York, NY.

Prospero, J.M., E. Bernatti, C. Schubert and T.N. Carlson, 1970: Dust in the Caribbean Atmosphere Traced to an African Dust Storm, Earth and Planetary Science Ltrs, 9, p. 287.

Selby, J.E.A. and R.A. McClatchey, 1976: Atmospheric Transmittance from 0.25 to 28.5 μm, Computer Code LOWTRAN 3B, AFGL Environmental Research Papers No. 587, AFGL-76-0258.

Tong, E.Y., G. Battel and R.B. Batchelder, 1976: Case Studies of Atmospheric Sulfate Distribution over the Eastern United States, Proc. Fifteenth Purdue Air Quality Conference, November 8-9, 1976, Indianapolis, IN.